Sedimentary evolution and effects of structural controls on the development of the Zambezi mixed turbidite-contourite system (Mozambique channel, southwest Indian Ocean) since the Oligocene

Ruth Fierens, L. Droz, Gwenael Jouet, M. Rabineau, F. Raisson, Nathalie Babonneau, Cécile Robin, S.J. J Jorry

Journal Pre-proof

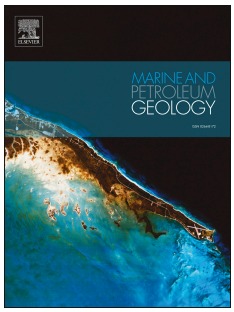

Sedimentary evolution and effects of structural controls on the development of the Zambezi mixed turbidite-contourite system (Mozambique channel, southwest Indian Ocean) since the Oligocene

R. Fierens, L. Droz, G. Jouet, M. Rabineau, F. Raisson, N. Babonneau, C. Robin, S.J. Jorry

PII: S0264-8172(22)00010-1

DOI: https://doi.org/10.1016/j.marpetgeo.2022.105532

Reference: JMPG 105532

To appear in: *Marine and Petroleum Geology*

Received Date: 6 September 2021

Revised Date: 24 December 2021

Accepted Date: 3 January 2022

Please cite this article as: Fierens, R., Droz, L., Jouet, G., Rabineau, M., Raisson, F., Babonneau, N., Robin, C., Jorry, S.J., Sedimentary evolution and effects of structural controls on the development of the Zambezi mixed turbidite-contourite system (Mozambique channel, southwest Indian Ocean) since the Oligocene, *Marine and Petroleum Geology* (2022), doi: https://doi.org/10.1016/j.marpetgeo.2022.105532.

Sedimentary evolution and effects of structural controls on the development of the Zambezi mixed turbidite-contourite system (Mozambique Channel, Southwest Indian Ocean) since the Oligocene

R. Fierens[1*], L. Droz[1], G. Jouet[2], M. Rabineau[1], F. Raisson[3],

N. Babonneau[4], C. Robin[5], S.J. Jorry[2]

1: CNRS, Université Bretagne Occidentale, Ifremer, Geo-Ocean, UMR6538, IUEM, 29280, Plouzané, France

2: Ifremer, Université Bretagne Occidentale, CNRS, Geo-Ocean, 29280, Plouzané, France

3: Clastic Sedimentology Group, TotalEnergies, 64000 Pau, France

4: Université Bretagne Occidentale, CNRS, Ifremer, Geo-Ocean, UMR6538, IUEM, 29280, Plouzané, France

5: CNRS, Géosciences Rennes, UMR6118, Université de Rennes, Rennes, 35042, France

*Corresponding author: ruth.fierens@univ-brest.fr

ABSTRACT

High-resolution multichannel seismic reflection data that spans significant parts of the Mozambique margin offshore the Zambezi River permits the study of the Oligocene to present architectural evolution of the Zambezi turbidite system. In this time frame, five major depositional units are recognized that evidence a widespread spatial and temporal occurrence of both turbiditic and contouritic sedimentation. They indicate that the sedimentary regime within the turbidite system changed from dominantly aggradational during the Oligocene to mainly erosional during Miocene to an interplay of erosional and depositional processes during the Plio-Quaternary. Different episodes of incision, linked with the Serpa Pinto, Angoche and Zambezi valleys, are recognized in the upstream portion of

the Zambezi Fan and highlight a westward (anticlockwise) shift of feeding axes. The central portion of the Zambezi Valley was affected by a progressive structural doming during the Miocene. The dominance of long-lasting erosional processes generated by the continuous rise of the seabed led to a deep entrenchment of the Zambezi Valley. This tectonically-controlled over-incision is believed to be the cause of the absence of Miocene levees, and has played an important role in the stabilization of the valley at its current position. Finally, our study revealed a quasi-constant development of contourite accumulations since the Late Miocene that occur most often synchronous with turbiditic sedimentation. The present study offers unique insight into the controls and stages of development of one of the largest turbidite systems in the world and demonstrates especially its susceptibility to structural activity.

Keywords: Zambezi turbidite system, Mozambique Channel, multichannel seismic profiles, turbidite, contourite, tectonic, Late Cenozoic

1. INTRODUCTION

Tectonic settings and sediment transfer are known to play an important role in the development and characteristics of deep-marine turbidite systems (Stow et al., 1985; Mutti and Normark, 1987, 1991). Besides possible regulation of upslope sediment flux and sediment delivery configuration (e.g. Stow et al., 1985; Reading, 1991; Reading and Richards, 1994), tectonics may deform basin floor topography and hence exert strong control on the morphodynamic evolution of a sedimentary system (Alexander and Morris, 1994; Bursik and Woods, 2000; Haughton, 2000; Morris and Alexander, 2003; Mayall et al., 2010; Howlett et al., 2020). Pre-existing features forming positive relief and/or tectonic movements (by faults, folds, salt or mud diapirs, salt walls, etc.) can disrupt the continuity of sediment flows and cause unusual geometries and sediment distribution patterns as they can lead to: (1) deflection, or the shifting of sediment routing due to an active structure (e.g., Tabernas-Sorbas Basin: Hodgson and Haughton, 2004; Niger Delta: Morgan, 2004; Angolan margin:

Gee and Gawthorpe, 2006); (2) diversion, when the gravity-driven processes change course because of a pre-existing structure (e.g., Makran margin: Kukowski et al., 2001; southern Barbados prism: Huyghe et al., 2004; Brazilian slope: Smith, 2004; offshore Tanzania: Maselli et al., 2020); (3) confinement, which indicates the restriction of turbidity currents by adjacent structures (e.g., Lower Congo Basin: Oluboyo et al., 2014; Levant Basin: Clark and Cartwright, 2009); or (4) blocking, where seafloor relief prevents sedimentation downstream of a structure (e.g., Gulf of Mexico: Rowan and Weimer, 1998; Beaubouef and Friedmann, 2000; Annot System: Sinclair and Tomasso, 2002; Fangliao Fan: Hsiung et al., 2018) of sediment pathways. Moreover, the crossing of a tectonic structure — which occurs if the erosional downcutting of sediment transport systems keeps pace with the rate of structural growth— can lead to a local or more extended topographic constriction of turbidity currents impacting flow behavior and sedimentation patterns (e.g., Gee et al., 2001; Morgan, 2004; Saller et al., 2004; Mayall et al., 2010). Although the principal anticipated response of deep-water gravity flows to structural elements are known, it is still a challenge to elucidate the depositional architectural evolution of extensive submarine turbidite systems to complex seafloor deformations.

The Mozambique Channel, hosting the Zambezi turbidite system, that has arisen from the break-up of Gondwana and the development of the East African rift system (e.g., Mougenot et al., 1986; Salman and Abdula, 1995; Calais et al., 2006; Leinweber and Jokat, 2012; Saria et al., 2014; Franke et al., 2015; Courgeon et al., 2018; Deville et al., 2018; Thompson et al., 2019) is known to be a tectonically dynamic region and hence, provides an interesting research area to explore the role of large-scale structural features and processes on the growth and evolution of a deep-water turbidite depositional system. Based on seismic reflection profiles, a number of previous studies on the Zambezi system have already hinted at a significant impact of morpho-tectonic features (i.e., Davie Ridge and Iles Eparses and seamounts) that caused the stable position of the Zambezi Valley and its resulting unusual deep entrenchment (Lort et al., 1979; Droz and Mougenot, 1987; Castelino et al., 2017). Unfortunately, the findings of these studies were hampered due to the low-resolution data

quality and/or insufficient seismic coverage. Other authors (e.g., Breitzke et al., 2017; Fierens et al., 2019; Miramontes et al., 2019) have suggested the important influence of oceanic bottom currents on the Zambezi Valley morphology. However, it seems unlikely to attribute the total deep entrenchment of the Zambezi Valley (~700 m; Fierens et al., 2019) merely to erosional activity of deep-water bottom currents (max. 500 m of incision; García et al., 2009; Van Rooij et al., 2010; Bozzano et al., 2021; Miramontes et al., 2021) and so it has not yet been possible to ascertain the precise cause of the deeply incised morphology of the Zambezi Valley. This study based on a new and extensive high-resolution seismic reflection dataset from the Zambezi depositional system seeks to improve our understanding of the regional sedimentary evolution. The main seismic facies and incisions are examined in order to explore and characterize the timing and extent of erosion and deposition in the Zambezi turbidite system from Oligocene to present-day. This specifically allows us to decipher which mechanisms are responsible for the exceptional deep entrenchment of the Zambezi Valley.

2. REGIONAL SETTING OF THE MOZAMBIQUE CHANNEL AND ZAMBEZI TURBIDITE SYSTEM

The Mozambique Channel is located in the western Indian Ocean between Mozambique (East Africa) and Madagascar (centered at 40°E and between 15°S and 42°S) (Fig. 1).

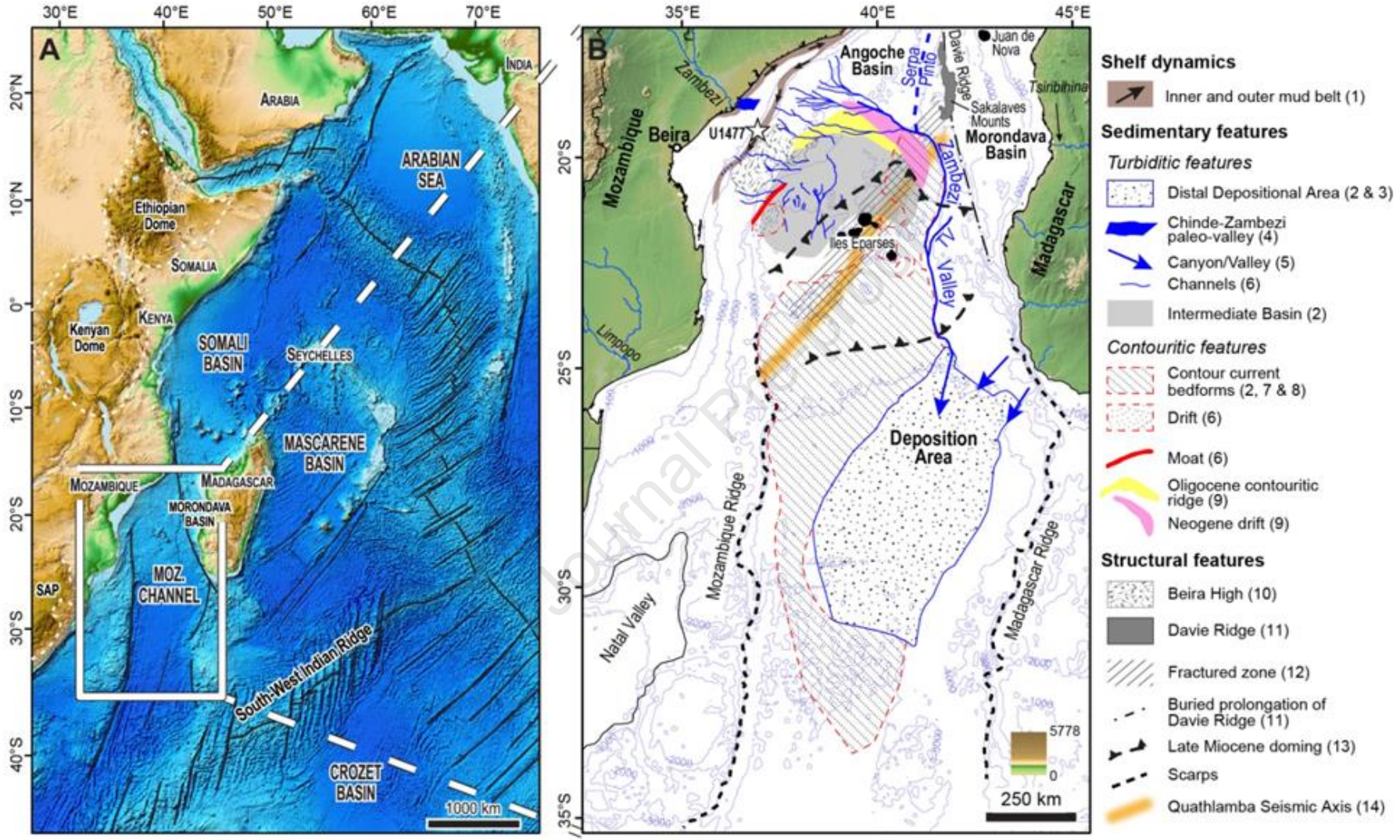
A
B
30°E
40°E
50°E
60°E
70°E
20°N
10°N
0°
10°S
20°S
30°S
40°S
INDIA
ARABIA
ARABIAN SEA
Ethiopian Dome
SOMALIA
KENYA
Kenyan Dome
SOMALI BASIN
SEYCHELLES
MASCARENE BASIN
MOZAMBIQUE
MADAGASCAR
MORONDAVA BASIN
MOZ. CHANNEL
SAP
South-West Indian Ridge
CROZET BASIN
1000 km
35°E
40°E
45°E
25°S
30°S
35°S
Zambezi
Angoche Basin
Serra Pinto
Davie Ridge
Juan de Nova
Tsiribihina
Mozambique
Beira
U1477
Sakalaves Mounts
Morondava Basin
Zambezi Valley
Madagascar
Iles Eparses
Limpopo
Deposition Area
Mozambique Ridge
Natal Valley
Madagascar Ridge
5778
0
250 km
Shelf dynamics
Inner and outer mud belt (1)
Sedimentary features
Turbiditic features
Distal Depositional Area (2 & 3)
Chinde-Zambezi paleo-valley (4)
Canyon/Valley (5)
Channels (6)
Intermediate Basin (2)
Contouritic features
Contour current bedforms (2, 7 & 8)
Drift (6)
Moat (6)
Oligocene contouritic ridge (9)
Neogene drift (9)
Structural features
Beira High (10)
Davie Ridge (11)
Fractured zone (12)
Buried prolongation of Davie Ridge (11)
Late Miocene doming (13)
Scarps
Quathlamba Seismic Axis (14)

99

Figure 1: (A) Location of the Mozambique Channel in the southwest Indian Ocean, with position of the main sedimentary basins, fracture zones (black lines) and continental elevation highs (white dotted lines) (modified from Delaunay, 2018; map from Amante and Eakins, 2009). SAP: South African Plateau. (B) Physiographic map of the Mozambique Channel showing main sedimentary and structural features (modified from Fierens et al., 2019). TV = Tsiribihina Valley. White star: core U1477 from IODP leg 361 (Hall et al., 2016). Compiled from published literature: (1) Schulz et al., 2011; (2) Fierens et al., 2019; (3) Kolla et al., 1980a; (4) Beiersdorf et al., 1980; (5) GEBCO, 2014; (6) Wiles et al., 2017; (7) Kolla et al., 1980b; (8) Breitzke et al., 2017; (9) Raisson et al., 2016; (10) Mahanjane, 2012; (11) Mahanjane, 2014; (12) Schematized from Courgeon et al., 2017, 2018; Deville et al., 2018 and Wiles et al., 2020; (13) Ponte, 2018, partly based on Baby, 2017; (14) Stamps et al., 2015.

2.1. Structural evolution

The formation of the Mozambique Channel was initiated in the Early Jurassic-Early Cretaceous during the breakup of the Gondwana (Salman and Abdula, 1995; Leinweber and Jokat, 2012; Thompson et al., 2019). Multiple rifting phases allowed the East Gondwana (Madagascar, Antarctica, India and Australia) to separate from the African block at ca. 165 Ma and slide southward along the transform Davie Fracture Zone (Fig. 1B) until around 120 Ma (Segoufin and Patriat, 1981; Coffin and Rabinowitz, 1987; Cochran, 1988; Gaina et al., 2015). During the Late Cretaceous (95 Ma) Madagascar separated from the Indian block (Salman and Abdula, 1995) and acquired its current position at 88 Ma (Late Cretaceous) (Reeves, 2014; Thompson, 2017). The East African continental margin underwent a period of stabilization during the Paleocene and the Eocene, until rifting resumed when the East African Rift System (EARS) developed (Salman and Abdula, 1995; Calais et al., 2006; Saria et al., 2014; Franke et al., 2015). The eastern branch of EARS initiated in the Oligocene (Dawson, 1992; Le Gall et al., 2008) and is prolonged offshore along the North Mozambique coastline and northern part of the Mozambique Channel (Mougenot et al., 1986; Franke et

al., 2015). This offshore rift segment is characterized by Neogene extension superimposed on earlier strike-slip structures of the Davie Fracture Zone (Rabinowitz et al., 1983; Reeves, 2014; Franke et al., 2015). A southwest prolongation of this offshore branch is argued by Courgeon et al. (2018), Deville et al. (2018) and Wiles et al. (2020) on the basis of a NNE-SSW densely distributed fault pattern, extending further south than the Sakalaves to the Mozambique Ridge on the East African Margin. These faults deformed the oceanic lithosphere of the Mozambique Channel in the same direction as the Agulhas-Falkland transform fault zone from at least Miocene times and are spatially associated to the Quathlamba active Seismic Axis (QSA) (Fig. 1B) (Stamps et al., 2015).

2.2. Present-day morphology and main morpho-tectonic features

The Mozambican shelf off the Zambezi River mouth gets connected to the deepest portions of the Mozambique Basin by the long and curvilinear Zambezi Valley that constitutes the main morphologic feature of the Zambezi Fan (Fierens et al., 2019) (Fig. 1). At present, no direct connection is known between the Zambezi River outlet and the Zambezi Valley. This submarine valley has a NW-SE orientation in its upper portion, transverse to the Mozambique Margin. It deflects towards the south when it approaches the Davie Ridge and passes through the Quathlamba Seismic Axis (Stamps et al., 2015) that is still active today (Courgeon et al., 2018; Deville et al., 2018; Wiles et al., 2020). The valley runs thereon between the Eparses carbonate platforms (Courgeon et al., 2016) to the west and the Madagascar margin to the east (Delaunay, 2018). At around 22°S, the Zambezi Valley coalesces with the Tsiribihina Valley (TV in Fig. 1B) that originates from the Western Madagascar margin. Approximately at the latitude of the southern tip of Madagascar the valley leads to a rather flat area constituting the Mozambique deep Basin. Between 22°S and 26°S, the valley crosses an elevated area that has undergone structural doming during the Late Miocene (Ponte, 2018).

The Davie Ridge is a 1200 km-long prominent N-S trending bathymetric high crossing the Mozambique Channel from the northeastern Mozambique to the southwestern Madagascar margin. It served as a morphological barrier for sediments originating from Madagascar, trapping the sediments in the Morondava Basin until the Miocene (23 Ma, Delaunay, 2018). Subsequently, this basin was filled in and allowed the Madagascar river inputs to overspill and contribute to the Zambezi Fan via the Tsiribihina Valley.

About 80 km off the Mozambican coast, the NE-SW Beira High (Fig. 1) forms a prominent basement high parallel to the Mozambique margin (Mahanjane, 2012; Mueller et al., 2016). This now buried structure is 300 km long and 100 km wide and served as a morphological barrier for sediments originating from the Mozambique margin until the Middle Miocene.

The central Iles Eparses are steep sloped carbonate platforms developed on top of volcanic edifices relating to an Oligocene to Early Miocene volcanic episode (Courgeon et al., 2016; Jorry et al., 2016). The Iles Eparses and the Beira High limit a small intraslope basin that has been named the “Intermediate Basin” (Fierens et al., 2019). This basin constitutes the more recent depositional system (Fierens et al., 2020).

2.3. Sediment sources

The Mozambique margin records a total sedimentary thickness of ca.6 stwt (~12 km) (Ponte, 2018; Ponte et al., 2019) and sediment deposition started at Early Cretaceous.

The main source of sediment filling the Mozambique Basin is the Zambezi River, which is with a catchment area of 1.3×10^6 km^2 the fourth largest river on the African continent (Fig. 2) (Thomas and Shaw, 1988; Walford et al., 2005; Milliman and Farnsworth, 2011).

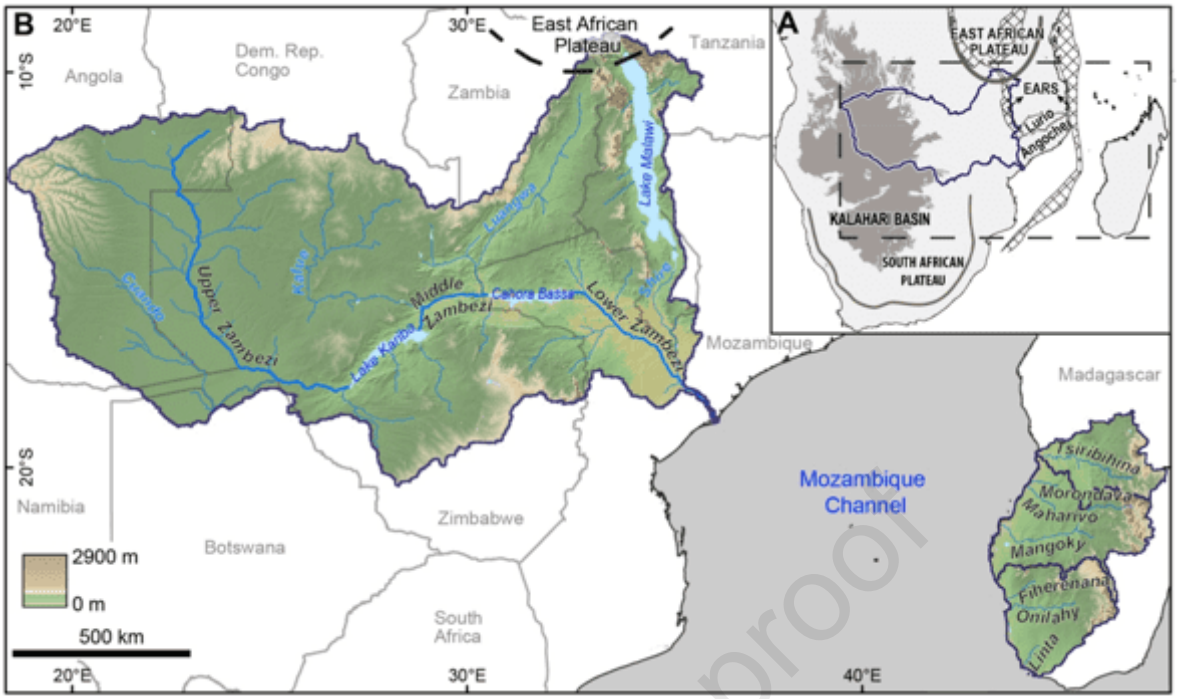

Figure 2: The Zambezi River and Madagascar Rivers catchments. (A) Position on the African continent (blue line) with indication of the major geomorphological and structural features (plateaus, basins, rift systems) (modified from Ponte, 2018; Courgeon et al., 2018; Deville et al., 2018). Cross design = rift systems and EARS = East African rift system. (B) Modern drainage system of the Zambezi, Tsiribihina, Mangoky and Onilahy rivers shown on topography (GEBCO, 2014). The Mongoky catchment area includes the Mangoky, Maharivo and Morondava rivers. The Onilahy catchment comprises the Onilahy, Linta and Fiherenana rivers.

The Zambezi River originates in central southern Africa and drains on its eastern portion major parts of the East African Rift System as well as the NE portion of the Kalahari Basin of the South African Plateau (Fig. 2A). It has had a polyphase evolution and has fed the Mozambican margin with fluctuating composition mixture of sediment (Garzanti et al., in press). The Zambezi River has a sediment load of 48 x 10^6 t/yr (Nugent, 1990; Milliman and Syvitski, 1992) and is 2,575 km long with a third of its length at an altitude higher than 850 m. From the African continent, two other important sources of sedimentary inputs have been observed: the Lurio (during Oligocene times) and Angoche (during Oligocene-Neogene period) watersheds (Fig. 2A). Western Madagascar rivers also contribute, but for a minor

194 amount, to the deposition in the Zambezi turbidite system (Fig. 2B). Madagascar sediment
195 inputs are originating mainly from the Tsiribihina River (525 km long, catchment area of
196 49,800 km^2) which is connected to the Zambezi Valley by the submarine Tsiribihina Valley.
197 The Mangoky River which drains the largest watershed in Madagascar (~55,750 km^2) is
198 probably also connected to this Tsiribihina Valley. The complex of Onilahy and Fiherenana
199 rivers directly feed the distal turbidite system in the deep Mozambique Basin.

200

201 **2.4. The Zambezi turbidite system**

202 The vast amounts of sediments discharged onto the Mozambican continental shelf by the
203 Zambezi River is attested by the very high sedimentation rate registered for the last climate
204 cycle by IODP drilling U1477 (about 1 m/kyr as a mean sediment rate for the last 120 kyr;
205 Leg 361, Hall et al., 2016) and during the Late Glacial Maximum (LGM, 26.5–20 ka BP) as
206 attested by the MOZ4-CS17 core (reaching about 2-3 m/kyr, Zindorf et al., 2021) both cores
207 retrieved on the upper slope in extension of the Zambezi Delta (Fig. 1B).
208 Fierens et al. (2019) showed that the fluvial input of the Zambezi River is deposited into two
209 main depocenters (Fig. 3) that together compose the Zambezi turbidite system: the Zambezi
210 Fan, which is fed by the 1500 km long entrenched Zambezi Valley that transfers sediments
211 to the deep basin in a vast zone of distal deposition (“Depositional Area”, Fig. 3) and a
212 Ponded Fan located in the Intermediate Basin, limited by the Mozambican slope and the Iles
213 Eparses.

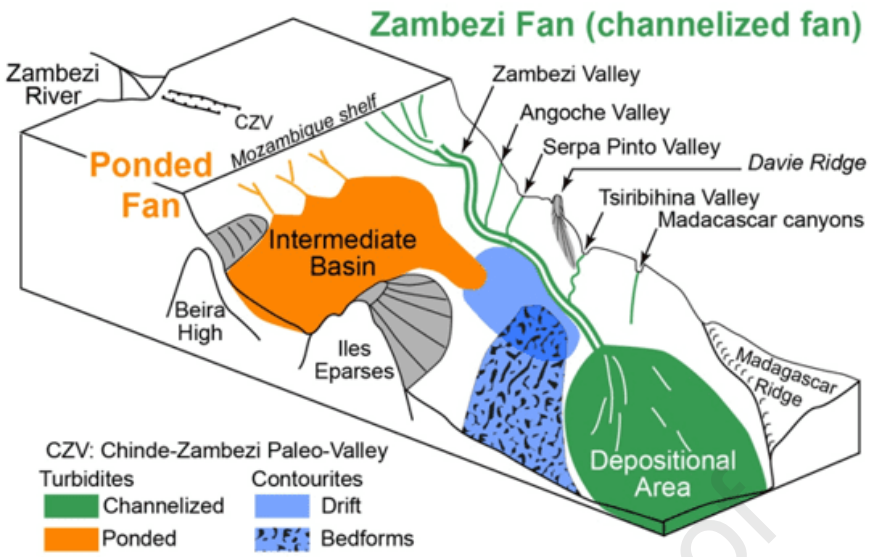

Figure 3: Major elements composing the Zambezi turbidite system (modified from Fierens et al., 2019).

The Zambezi Fan has been studied previously by multiple studies (e.g., Simpson, 1974; Kolla et al., 1980a, 1980b; Droz and Mougenot, 1987; Breitzke et al., 2017; Wiles et al., 2017a; Miramontes et al., 2019; Fierens et al., 2019, 2020). From these we know that the Zambezi Valley and the distal Depositional Area are characterized by coarse-grained deposits (Simpson, 1974; Kolla et al., 1980b; Fierens et al., 2019). The presence of sediment waves (Breitzke et al., 2017; Fierens et al., 2019) and the flank erosion of the Zambezi Valley (Miramontes et al., 2019) reveal important sediment reworking by strong bottom currents. In contrast, the Ponded Fan has been more poorly studied (Wiles et al., 2017b; Fierens et al., 2019, 2020). Based on sub-bottom profiler data, Fierens et al. (2019) suggested that the Ponded Fan mainly consists of fine-grained turbidites with thin sheet-like, coarse-grained interbeds.

The current Zambezi Fan was established from Oligocene times when the Zambezi Delta progradation was initiated (Droz and Mougenot, 1987; Ponte, 2018). Since then, large quantities of sediment have been drained from the Zambezi watershed causing a substantial progradation of the Mozambique shelf (Walford et al., 2005; Ponte et al., 2019) (Fig. 4).

During Pleistocene times, the continental margin progradation was most important and mass transport activity was common (Ponte et al., 2019).

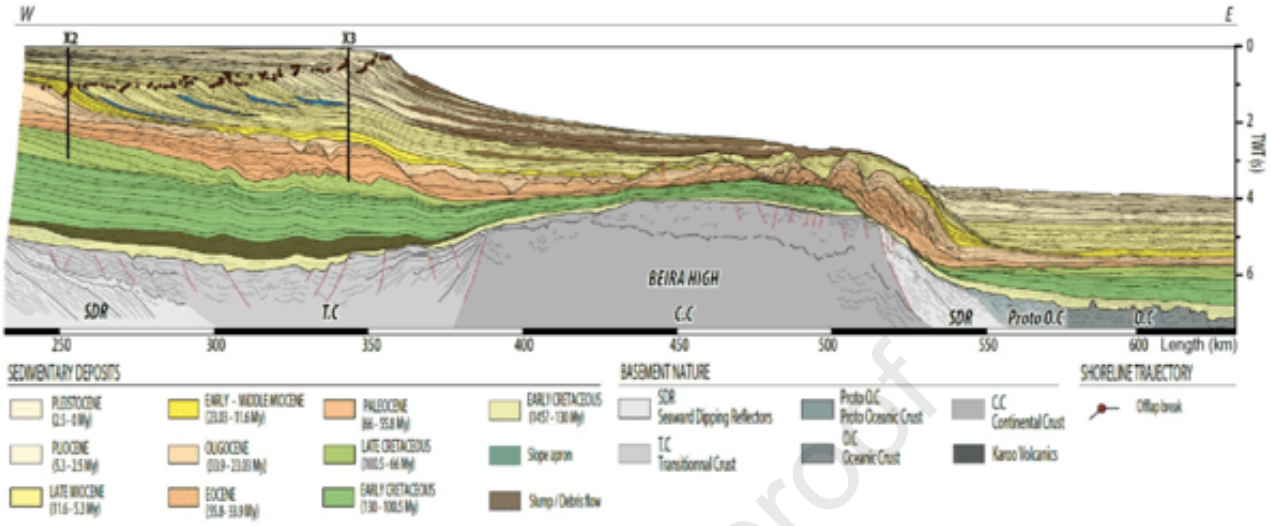

Figure 4: Stratigraphic architecture of the Mozambique margin (Ponte et al., 2019) (see location on Fig. 5).

The architecture of the Zambezi Fan is poorly known, except for the feeding axes of the fan. Droz and Mougenot (1987) have shown that the initiation of the Zambezi Fan, during Oligocene times was related to the Serpa Pinto Valley, a N-S feeding axis close to the Davie Ridge (Figs. 1, 3). This valley received sedimentary inputs from the Lurio catchement (Roquette, 2016; Ponte, 2018) (Fig. 2A). The shift to the present-day NW-SE Zambezi Valley occurred in the Mid-Miocene possibly in response to tectonic activity induced by the development of the East African Rift System that affected the northern Mozambique margin. Ponte (2018) indicates that during Oligocene-Neogene times, sediments were supplied by the Angoche (Fig. 2A) and Zambezi watershed by several channeling systems that join the Serpa Pinto Valley (Oligocene) and later the Zambezi Valley (from Middle Miocene). Since the Middle Miocene, sediments from Madagascar contributed to the feeding of the Zambezi system (see section 2.2), funneled in the Tsiribihina Valley (Delaunay, 2018).

3. MATERIAL AND METHOD

This work is based mainly on high-resolution seismic data that were acquired during three cruises carried out as part of the PAMELA (PAssive Margin Exploration LAboratories) project

(Bourillet et al., 2013): PTOLEMEE (Jorry, 2014), PAMELA-MOZ2 (Robin and Droz, 2014) and PAMELA-MOZ4 (Jouet and Deville, 2015) (Fig. 5). The PAMELA data are unevenly distributed across the study area with a majority located around the Zambezi Valley (Fig. 5A). The seismic lines are more dispersed on the Mozambican continental slope (N to NE of Iles Eparses) and in the distal Mozambique Basin.

On the Mozambican slope, the dataset was complemented with seismic data made available by Total. Additional seismic data from the MD163-MoBaMaSiS expedition (Reichert and Aslanian, 2007) were also used.

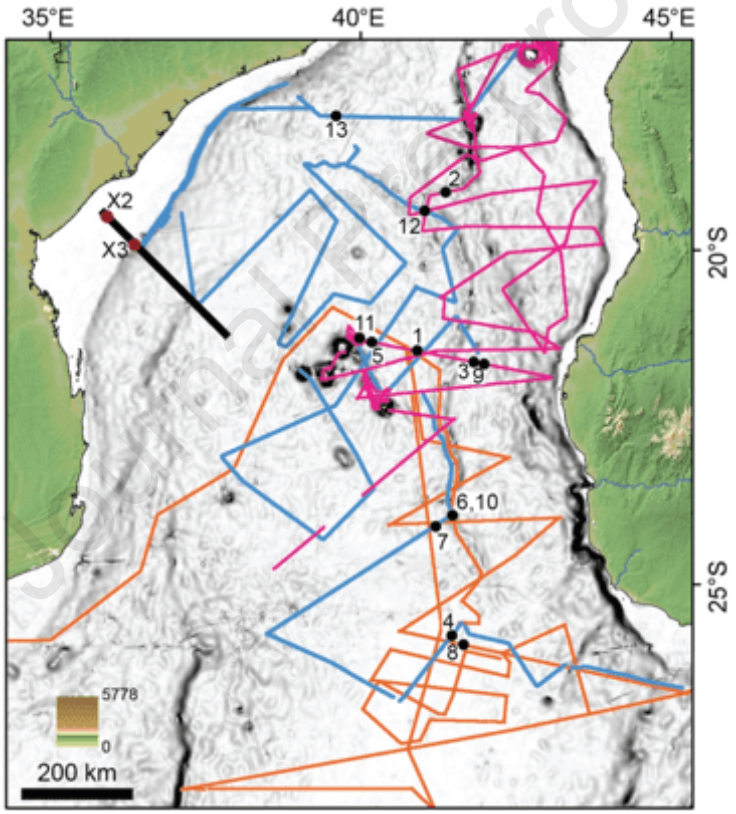

Figure 5: Data used in this study. PAMELA high-resolution multichannel seismic data set. Magenta lines: PTOLEMEE cruise (Jorry, 2014); orange lines: MOZ2 cruise (Robin and Droz, 2014); bleu lines: MOZ4 cruise (Jouet and Deville, 2015). Thick black line: position of the seismic line with industrial wells (X2, X3) presented in Fig. 4 (Ponte, 2018). 1 to 13: location of the seismic facies examples shown in Fig. 6.

3.1. PAMELA seismic data acquisitions

272 This study used approximately 23,000 km of multichannel seismic data (Fig. 5) that were
273 acquired aboard of the L'Atalante and Pourquoi Pas? research vessels. The key parameters
274 of the seismic acquisitions are given in Table 1. The multichannel seismic data image the
275 sediment cover up to ca. 2–3 seconds two-way time (stwt), depending on the nature of
276 deposits and the bathymetric conditions.
277

Cruise	PTOLEMEE and MOZ2	MOZ4
Source	2 GI guns (105 and 45 ci)	2 GI guns (105 and 45 ci)
Receiving device	streamer 24 traces	streamer 48 traces
Acquisition speed	8-10 knots	8-10 knots
Inter shot	10 s (50 m at 10 knots)	10 s (50 m at 10 knots)
Vertical resolution	~15 m	~5 m

Table 1: Acquisition parameters of the high-resolution multichannel seismic systems used during the PTOLEMEE, PAMELA-MOZ2 and PAMELA-MOZ4 cruises.

3.2. PAMELA data processing

The seismic data were processed using Ifremer in-house softwares Qc-SISPEED© (PTOLEMEE, MOZ2) and SolidQC© (MOZ4). The processing sequence includes quality controls of navigation and seismic data, binning, SEGD to SEGY format conversion, pass-band filtering (15-150 Hz), correction of source delay and stacking and migration at constant velocity (1500 m/s).

3.3. Seismic data interpretation

Seismic interpretation was performed following the seismic stratigraphy principles (Mitchum et al., 1977). This approach involves the recognition and correlation of seismic units (definition according to Mitchum and Vail, 1977) complemented by an analysis of the seismic facies. The limits of these units are recognized by reflection terminations (onlaps, downlaps, erosional truncations, and toplaps). The geometry of reflections within an individual seismic unit is described using seismic facies analysis. Seismic facies are defined by looking at the internal and external configurations of the seismic units. Internal reflection characters are described by the continuity, amplitude, frequency and geometry of the reflections. The upper and lower boundaries of the seismic facies define its 2- or 3-dimensional external shape (e.g.

300 wedge, lens or sheet geometry). The stratigraphic framework established by Ponte (2018) on
301 the Mozambique margin (Fig. 4) served as a basis for our study.
302 The processed data (navigation and SEGY seismic files) were imported into the IHS
303 Kingdom Suite® software that was used to display and analyze the data. Isopach maps were
304 created with grid cell sizes of 200x200 m and produced in second two-way travel-time (stwt).
305 A time-depth conversion is provided using an approximate velocity of 2000 m/s (Ponte,
306 2018). With regard to the large size of the study area and the generally low density of the
307 seismic data, the interpolation of seismic interpretations has been locally difficult. We have
308 chosen to downgrade the isopach maps by showing a maximum of five classes of thickness
309 (0.015-0.25, 0.25-0.5, 0.5-0.75, 0.75-1.0 and 1.0-1.634 stwt). The lowest value (0.015 stwt)
310 corresponds to the vertical resolution of the seismic data with the lowest resolution
311 (PTOLEMEE and MOZ2 data, see Table 1). These isopach maps were displayed by using
312 ArcGIS® v10.3.1 (World Mercator map projection).
313

314 **4. RESULTS AND INTERPRETATION**

315 **4.1. Seismic facies and process-based interpretation**

316 The high-resolution multichannel (24- and 48-channels) seismic profiles of the Mozambique
317 Channel reveal three main types of seismic facies that are those typically encountered on
318 continental margins and in turbidite systems (e.g., Winker, 1996; Piper et al., 1999;
319 Babonneau et al., 2002; Adeogba et al., 2005): stratified (S), chaotic (C) and transparent (T)
320 facies. Main characteristics of the facies are summarized in Table 2 and examples are
321 provided in Fig. 6.

Facies class		Facies characters	Sub-class	Configuration	Location	Interpretation
STRATIFIED	**S1**	High Co, Low to medium A, High F	***S1a***	Parallel, or bi-directionally convergent with undulations	Right hand-side of the Zambezi Valley	Contourite drift
			S1b	Uni-directionally convergent away from a valley or channel axis	Left hand-side of the Zambezi Valley and levees of distal channel-levees	Fine-grained overspill turbidites alternating with very fine hemipelagic deposits
	S2	High Co, High A, High F	***S2***	Parallel and onlaping (infilling)	Distal Intermediate Basin	Alternation of hemipelagic deposits and sheet-like turbiditic sediments
	S3	High Co, High A, Low F	***S3a***	Parallel (infilling valleys/depressions)	Zambezi Valley fill	Coarse-grained turbidites
			S3b	Parallel, wide extension	Right hand-side of the Zambezi Valley	Coarse-grained turbidites
CHAOTIC	**C**	Low Co, High A, Low F	***Ca***	Basal unconformity, flat topped lens shape	Madagascar margin and distal Depositional Area of the Zambezi Valley	Coarse-grained distal turbidites
			Cb	Contorted and divergent from valley walls	Zambezi Valley fill	Slumped coarse-grained deposits
			Cc	Contorted	Eparses hills and sea-mounts	Carbonate deposits
TRANSPARENT	**T**	Very low A and F	***Ta***	Entirely transparent, isopach	Inside the Zambezi Valley	Mass-transport deposit
			Tb	Some contorted reflections	Mozambique slope, Zambezi Valley, distal Depositional Area and Intermediate Basin	Mass-transport deposit

322 Table 2: Description and interpretation of the seismic facies encountered in the Zambezi
323 turbidite system. Facies characters are described in term of the continuity (Co), amplitude (A)
324 and frequency (F) of the reflections.

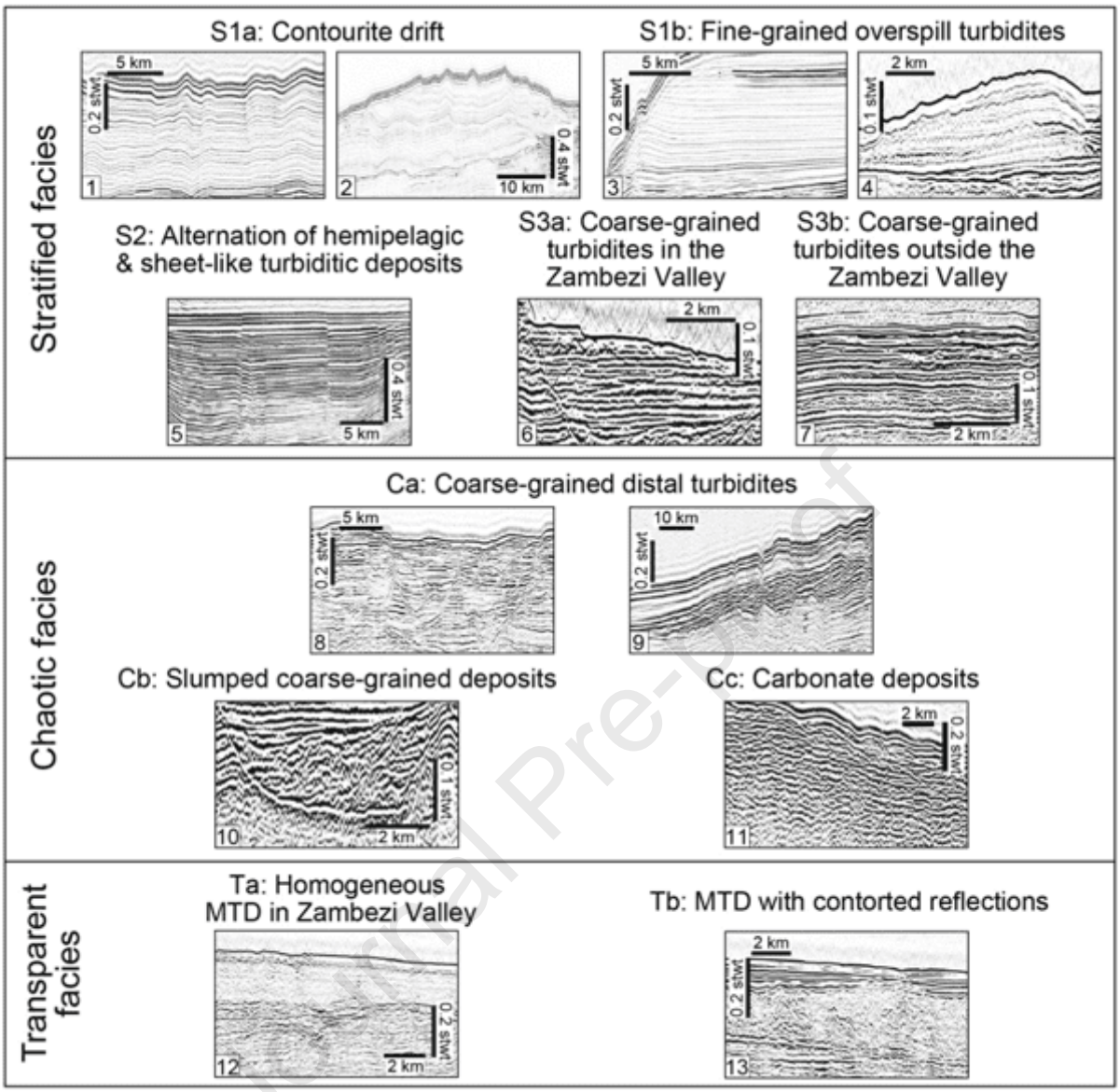

Figure 6: Examples of the seismic facies encountered in the Zambezi turbidite system (location of line portions is shown in Fig. 5 as black dots 1 to 13).

The stratified facies (S) are the most common and widespread facies identified in the Mozambique Channel. Their main characteristic is a generally good continuity of the reflectors that may be planar or undulated. Variations in amplitude, frequency and configuration led to recognize contouritic deposits (S1a), fine-grained overspill turbidites (S1b), alternating hemipelagic and sheet-like turbiditic deposits (S2) and coarse-grained turbidites (S3a and S3b).

The chaotic facies (C) are characterized by contorted reflections with low continuity and by frequent erosional features and local unconformities. The Ca facies are widely observed at

the distal end of the Zambezi Valley where coarse-grained sediments dominate (Kolla et al., 1980a, b). In addition, local flat top lens-shaped seismic units are identified on the Madagascar slope where it is thought to image coarse-grained turbidites. The chaotic facies are also observed as contorted reflections that are tilted towards the valley axis (Cb), which are interpreted as slumped deposits from the valley flanks in agreement with the interpretation of other authors (e.g., Deptuck et al., 2003; Janocko et al., 2013). At the foot of the seamounts of the Iles Eparses, the Cc chaotic facies is interpreted as carbonated turbidites with hemipelagic muds (Counts et al., 2018).

The transparent facies (T) are observed as homogeneously transparent inside the Zambezi Valley (Ta) or as mostly transparent with faint and contorted reflections at various sites of the Mozambique margin and basin (Tb). These facies are usually interpreted as mass-transport deposits (MTDs) (e.g., Imbo et al., 2003; Garziglia et al., 2008; Loncke et al., 2009; Dennielou et al., 2019; Badhani et al., 2020).

4.2. Architecture and stratigraphy of the Zambezi turbidite system

4.2.1 The Mozambique Basin feeding networks

The PAMELA data with a water depth up to 2500 m and data from Total between 2500 m and 1000 m water depth show that the upper portion of the Zambezi Valley (i.e. most northwestern part) has been fed by two main converging tributary networks (Fig. 7A), the youngest Northern and the oldest Southern Zambezi network (Fierens et al., 2019). Tributaries of these networks do not show clear connections to the upper slope and disappear halfway up the slope. The absence of connection to the uppermost slope is not due to a lack of data, but rather because of the absence of lasting incisions upstream of the slope. The Intermediate Basin, in contrast, was fed by a loose network of parallel valleys distributed homogeneously along the Mozambique slope (black lines in Fig. 7A).

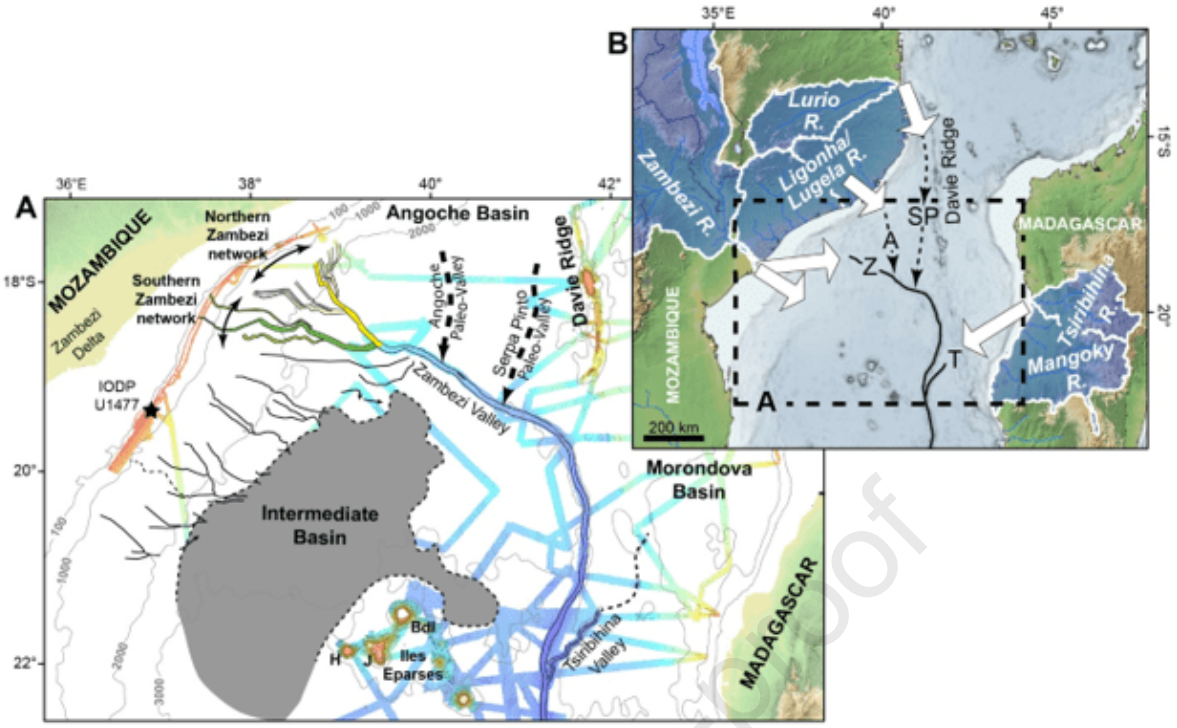

Figure 7: Marine feeding axes of the Zambezi turbidite system and continental sediment sources. (A): Various submarine networks of the Zambezi Fan (Northern and Southern Zambezi networks, Angoche and Serpa Pinto paleo-valleys and Tsiribihina Valley) and the ponded turbidites accumulated in the Intermediate Basin. BdI: Bassas da India, H: Hall Bank, J: Jaguar Bank. (B): Main rivers feeding the Zambezi turbidite system (rivers watersheds from http://www.fao.org/geonetwork, 2019). Z: Zambezi Valley; T: Tsiribihina Valley; A: Angoche Paleo-Valley; SP: Serpa Pinto Paleo-Valley.

Downstream, the Zambezi Valley receives three main tributaries on its left hand-side: the Angoche, Serpa Pinto and Tsiribihina valleys (Fig. 7A). The valley that originates northwards from the Angoche Basin is referred to as the Angoche Valley in this paper. The Serpa Pinto Valley (Droz and Mougenot, 1987) originates from the Lurio watershed and possible other northeastern African drainage basins (Ponte, 2018) and runs adjacent to the Davie Ridge. These two paleo-tributaries have a North-South orientation and provided sediments from the Northern Mozambique rivers to the Zambezi Fan (Fig. 7B). The Tsiribihina Valley originates from the Western Madagascar margin (Tsiribihina and Mangoky drainage basins) and is currently providing sediments to the lower portion of the Zambezi Fan.

381

382 4.2.2. Seismic units

383 Based on the seismic facies analysis and interpretation (see Section 4.1) we identified four
384 main facies types: fined-grained overbank turbidites (lateral levees), coarse-grained
385 turbidites (mainly channel fills or lobe complexes), fine-grained contourites (drifts) and mass-
386 transport deposits (MTDs, restricted in valleys or more widespread in the distal depositional
387 area) (Fig. 8). These facies are organized into five main seismic units (U1 to U5) that are
388 regionally correlated (Fig. 8A, 9). U1 to U4 are stacked up in the Zambezi Fan, while U5
389 corresponds to the Ponded Fan in the Intermediate Basin. Figure 10 shows the thickness
390 maps (in sec TWT) of the 5 units that could be correlated throughout the study area.
391 Additional units (Ua to Ug on Figs. 8A, 9) are observed locally in the Zambezi Fan, but the
392 low density of seismic data prevents their correlation and they are not considered in this
393 paper.
394 Towards the distal depositional area (Fig. 8B), we could not individualize U1 to U4, therefore,
395 a single 1000 m-thick seismic unit called Depositional Area (DA) has been considered in this
396 area.

397

398

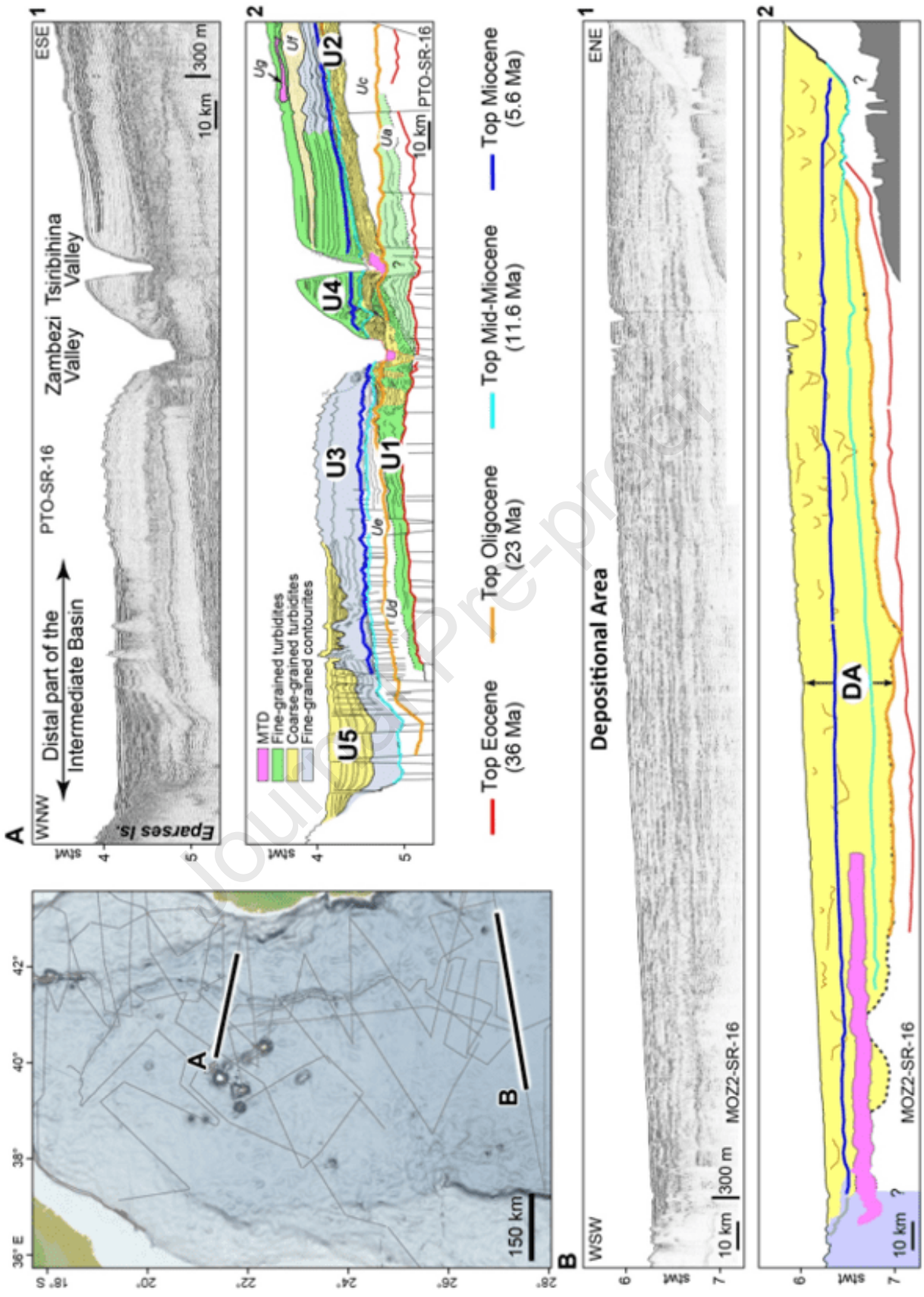

Figure 8: Seismic sections (with their location) illustrating the seismic facies, the regional seismic units and Ponte's (2018) stratigraphy found upstream (A) and downstream (B) of the Zambezi turbidite system.

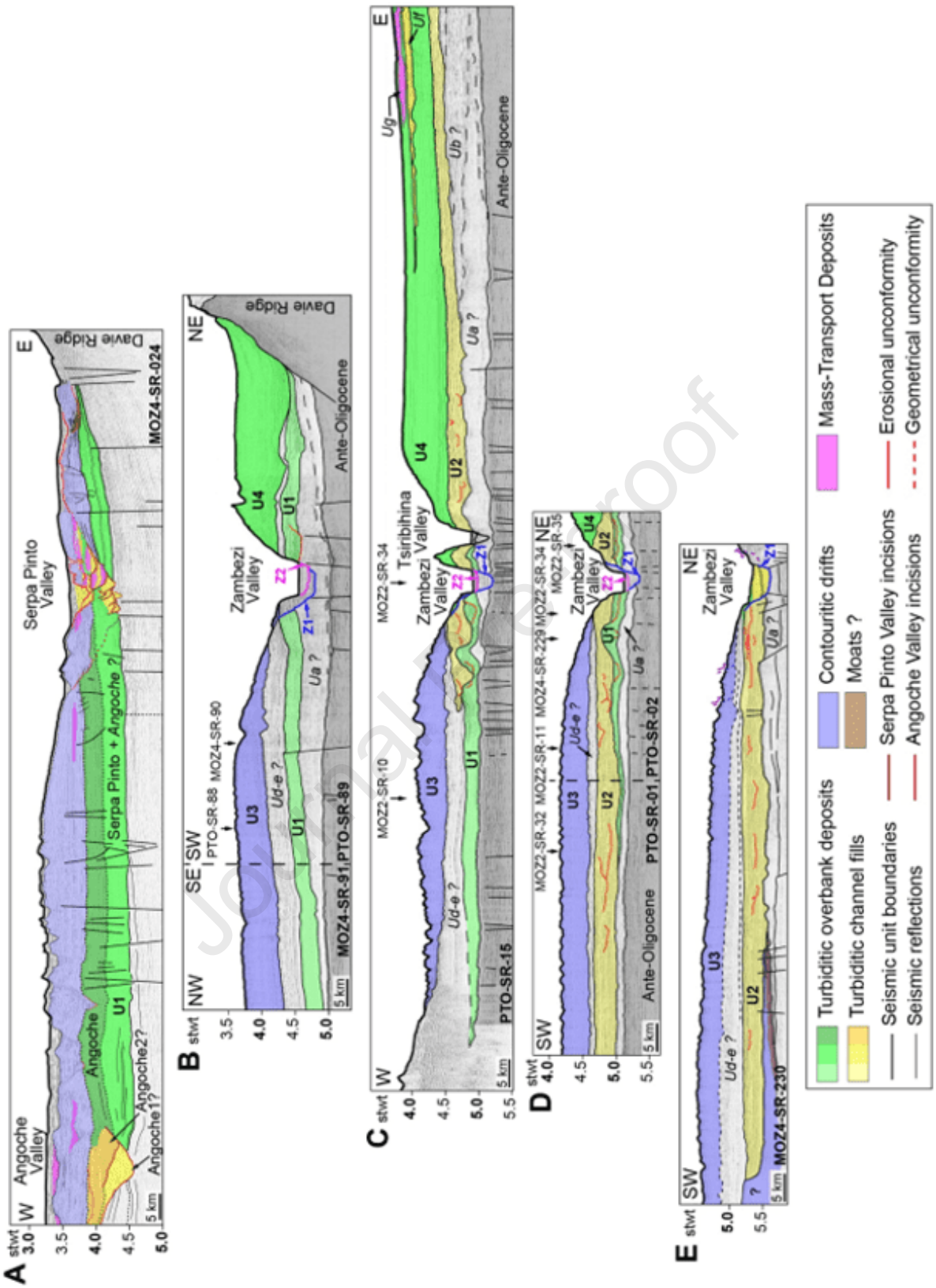

Figure 9: Interpreted seismic reflection profiles from north (A) to south (E) showing the major sedimentary evolution of the Zambezi turbidite system (see supplementary material A for uninterpreted profiles). Z1 and Z2 denote the main incisions of the Zambezi Valley. See Fig. 10A for location of the seismic profiles.

408

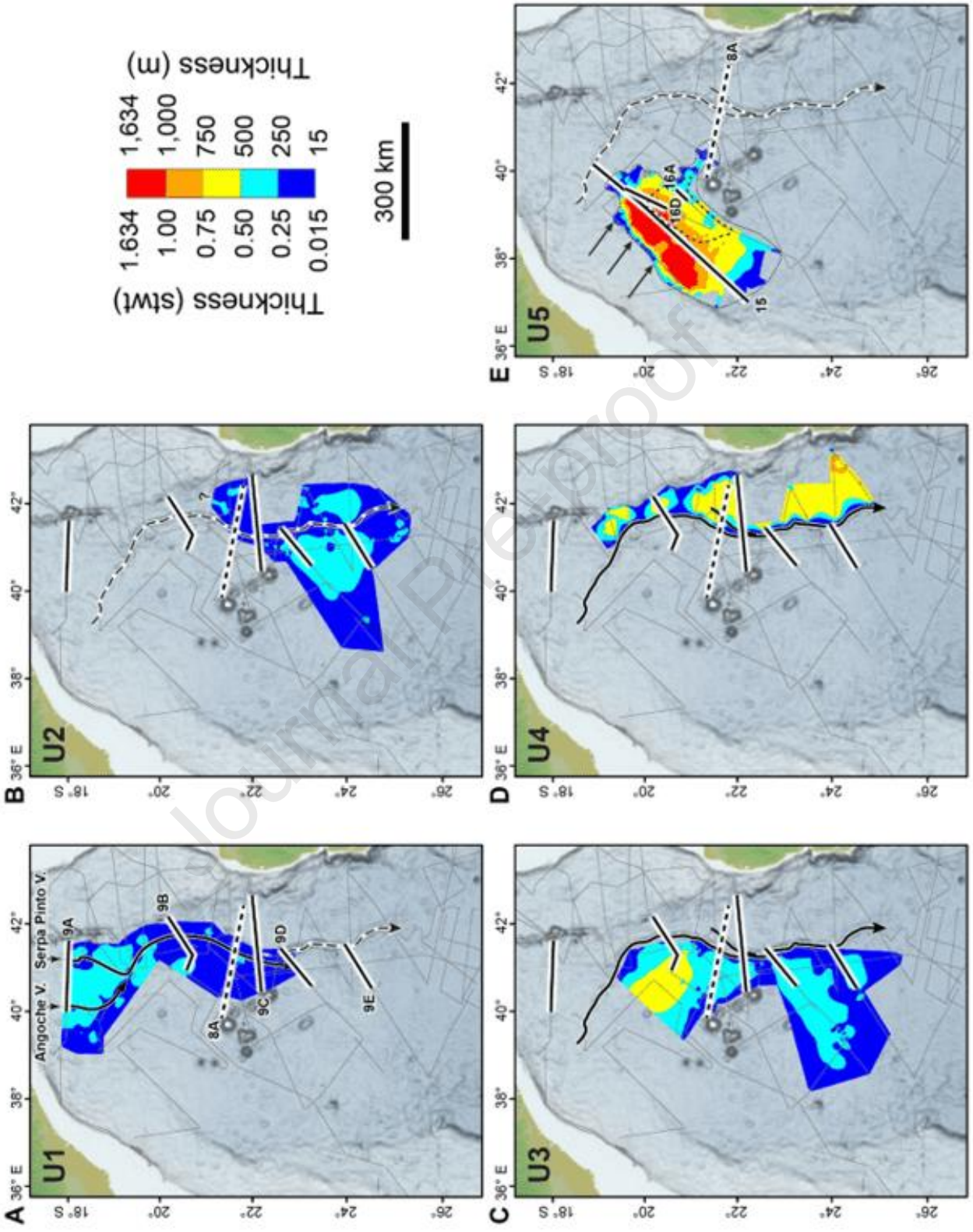

409

410 Figure 10: Distribution and thickness of the five seismic units of the Zambezi turbidite system
411 (Zambezi Fan, U1 to U4, and Ponded Fan, U5). The position of the Zambezi Valley is
412 indicated either as a dashed line when inactive (A, B, E) or as a continuous black line when

active (C, D). The possible course of the Angoche and Serpa Pinto Valleys is additionally shown in A. Straight black and dashed lines are the location of seismic profiles of Figs. 8, 9, 15 and 16.

4.2.3. Sedimentary evolution of the Zambezi turbidite system

A general spatial overview (from north to south) of the architecture of the Zambezi Fan with the distribution of the seismic units is provided in figure 9. The distribution and isochore maps of the five main seismic units are provided in figure 10.

Unit U1: Channel-Levee Complex

Unit U1 (Figs. 8A, 9) is wedge-shaped and composed of the association of high-amplitude channel infilling facies (S3a) interpreted as coarse-grained turbidites and lateral low to medium amplitude, high-frequency S1b facies interpreted as fine-grained turbidites (Fig. 6 and Table 2). The convergent configuration distally from the valley is typical of overbank deposits (levees).

Unit U1 originates in the northern most part of the study area, in relation with the N-S oriented Serpa Pinto and Angoche valleys (Fig. 10A). The depositional history of the Serpa Pinto Valley appears especially complex with multiple episodes of cut-and-fill in link with overbank deposition and intercalated with small mass-transport deposits inside the channels (Fig. 11). Consequently, U1 is interpreted as a channel-levee complex comprising several channel-levee systems. Available data are too limited to allow an extensive interpretation of the activity of this valley, and therefore it has been considered as a thick single event in this study. In addition, in this northern area, overbank deposition from both the Serpa Pinto Valley to the east and the Angoche Valley to the west indicates that both valleys have been active synchronously and served as feeding axes to the so called Serpa Pinto channel-levee Complex (Fig. 9A, 10A).

U1, including the Angoche contribution, shows its maximal lateral extent (approximately 260 km) and thickness (0.5 stwt, i.e. ~500 m) in the upstream northern part (Fig. 10A). Close to

441 the Davie Ridge a significant contribution of contouritic sedimentation led to the deposition of
442 thick contouritic drifts (S1a in Figs 6 and 9A).
443 The basal channels of the Serpa Pinto and Angoche Valley show limited erosion in the
444 Eocene-Oligocene strata, and appear as a flat and wide erosional unconformity (Fig. 11).
445 Downstream the confluence with the Zambezi Valley (Fig. 8A, 9B to 9D), the Serpa Pinto
446 Valley is more deeply incised, and disappears downstream because of over-incision of the
447 Zambezi Valley (see Section 4.2.4). Where the channels are still observed they are filled in
448 with typical channel infilling facies, i.e. discontinuous, high-amplitude and low-frequency
449 reflections (S3b in Fig. 6). The distribution of unit U1 (Fig. 10A) shows an approximate N-S
450 direction. The channels appear relatively close to the present-day position of the Zambezi
451 Valley except in the downstream extension of Unit U1 where they diverge toward the west
452 (Fig. 10A). U1 is identified and correlated downstream to a latitude just a bit further south
453 than the Tsiribihina confluence (Fig. 10A), however, the downstream extension of this unit
454 remains uncertain.

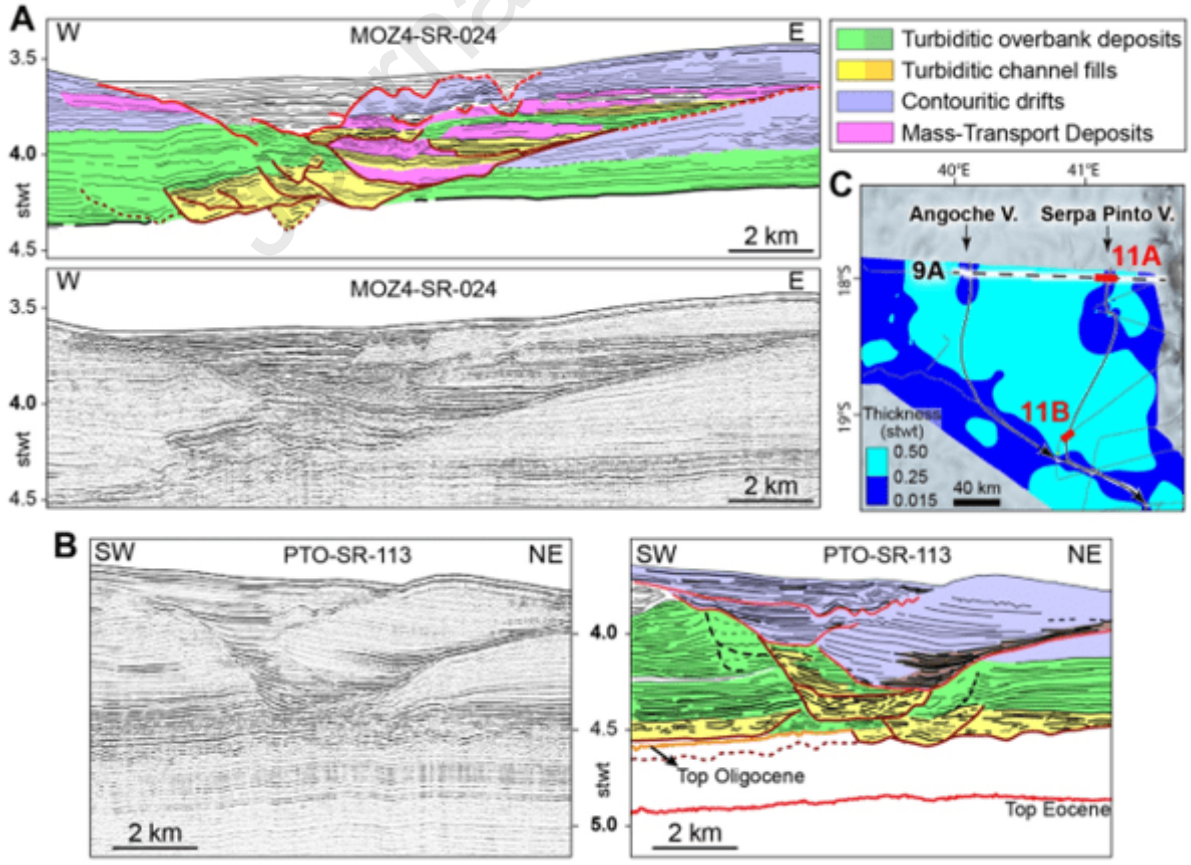

455

Figure 11: The Serpa Pinto Valley depositional succession. (A): Close up of seismic profile MOZ4-SR-24 (shown in Fig. 9A) illustrating the northern portion of the Serpa Pinto Valley. (B): Seismic profile PTO-SR-113 showing the southern portion of the Serpa Pinto Valley, close to the confluence with the Zambezi Valley. C: Close up of the distribution and isochore map of unit U1 (see Fig. 10A) showing the location of seismic lines A and B.

Unit U2: Lobe Complex

Unit U2 consists mainly of S3b facies (continuous, high-amplitude, low frequency reflections, with frequent local erosional unconformities) (Fig. 8 A, 9C-E) and is interpreted as coarse-grained turbidites.

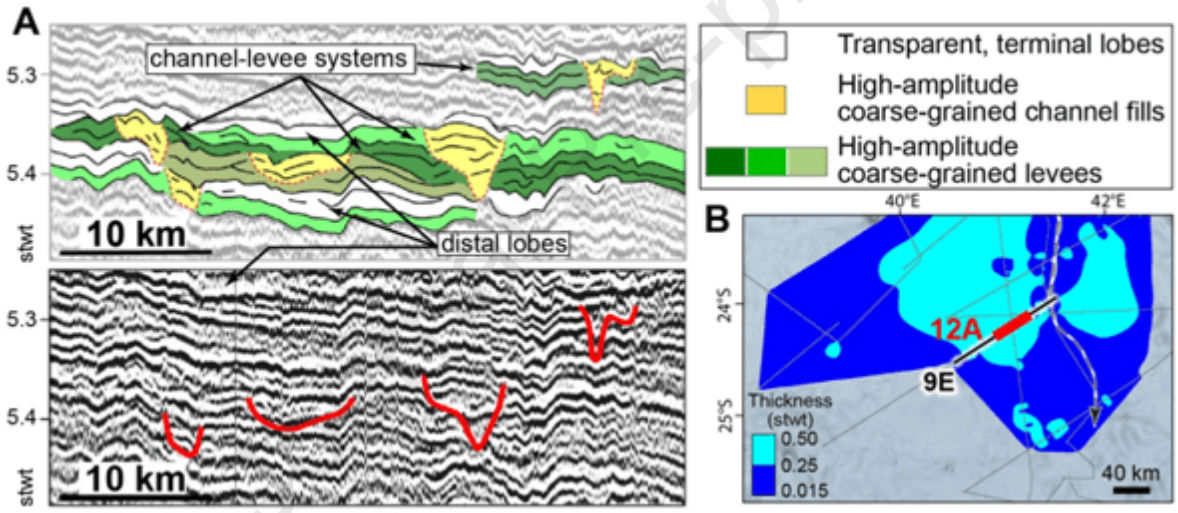

Figure 12: (A): Close-up of unit 2 showing the possible stacking of small coarse-grained channel-levee systems (seismic profile MOZ4-SR-230, Fig. 9E). (B): Zoom of the distribution and isochore map of unit U2 (see Fig. 10B) showing the location of seismic profile A.

The detailed internal organization of this high-amplitude unit (Fig. 12) reveals ca. 0.03 stwt (~ 30 m) thick wedge-shaped seismic bodies lateral to channel-like erosional features, evoking small and coarse-grained channel-levee systems which are stacked up in the dominantly high-amplitude facies. More continuous high-amplitude reflections and transparent levels intercalated with the channel-levee systems evoke coarse-grained sheet-like turbidites and

terminal lobes, respectively. These seismic characteristics suggest that unit U2 is composed of channel-mouth deposits, distinctive of distal depositional environments.

The distribution of unit U2 (Fig. 10B) shows a pear shape with an average NE-SW orientation, i.e. oblique to the current Zambezi Valley (Fig. 10). This unit is up to 0.4 stwt thick (~400 m, Fig 10) and is generally widespread (up to ~330 km of lateral extent in its downstream portion, on Fig. 10B), more developed at the right hand-side of the Zambezi Valley. At its northeastern limit, unit U2 is mainly recognized on the left hand-side of the Zambezi Valley (Fig. 8A). Based on available data, it was not possible to extend this unit more to the north, so that we may only hypothesize on its origin (see Section 5.1). The southern limit of U2 extends more distally compared to unit U1. U2 is incised by the paleo-incisions of both the Zambezi and Tsiribihina Valley (Figs. 8A, 9E), which might indicate that unit U2 pre-existed the development of these valleys or that the incision of these valleys has endured after the deposition of U2.

Unit U3: Contourite drift on the western side of the Zambezi Valley

Unit U3 (Figs. 8A; 9) is composed of continuous low-amplitude, mostly high-frequency reflections (facies S1a). This unit is up to 0.7 stwt (~ 700 m) thick and shows a slightly domed wedged shape with bidirectional thinning. Close to the Zambezi Valley, the lateral thinning is partly due to erosion on the Zambezi Valley flanks. Reflections are parallel under the thickest part of the wedge and are affected by sediment bedforms that are observed in the whole vertical extent of the unit (Figs. 9, 13A). These bedforms, observed on bathymetric and sub-bottom profiler data (Fierens et al., 2019) are interpreted as bottom current controlled sediment waves. Based on the shape, the internal configuration and the similarities with other contourite drifts identified in the Mozambique Channel (Fig. 13B) or in literature (Hernández-Molina et al., 2010; Miramontes, 2016), U3 is interpreted as a contourite drift. Westward at the distal and basal limit of the Intermediate Basin, approaching the Iles Eparses, unit U3 appears to be locally structured by high reliefs wherein reflections are lost and the facies becomes mostly transparent (Fig. 8A). These reliefs are associated to a dense

network of faults (Deville et al., 2018), mainly observed in the underlying units (Ud and Ue) and evoke structural domes (associated to volcanism?).

Closer to the Iles Eparses seamounts, high-amplitude reflections are intercalated in the dominantly low-amplitude facies. They could represent detrital carbonate sediments originating from the islands, synchronous with the contourite deposition (Counts et al., 2018).

Unit U3 is solely observed along the right (looking downstream) border of the Zambezi Valley (Fig. 10C) and is locally less developed towards the SE of Iles Eparses (Fig. 13C). The width of the contourite drift reaches up to ~300 km (Fig. 10C) and the unit is recognized along at least 680 km from upstream to downstream. It is important to note that the northwestern and southern limits of unit U3 remain uncertain due to the lack of data.

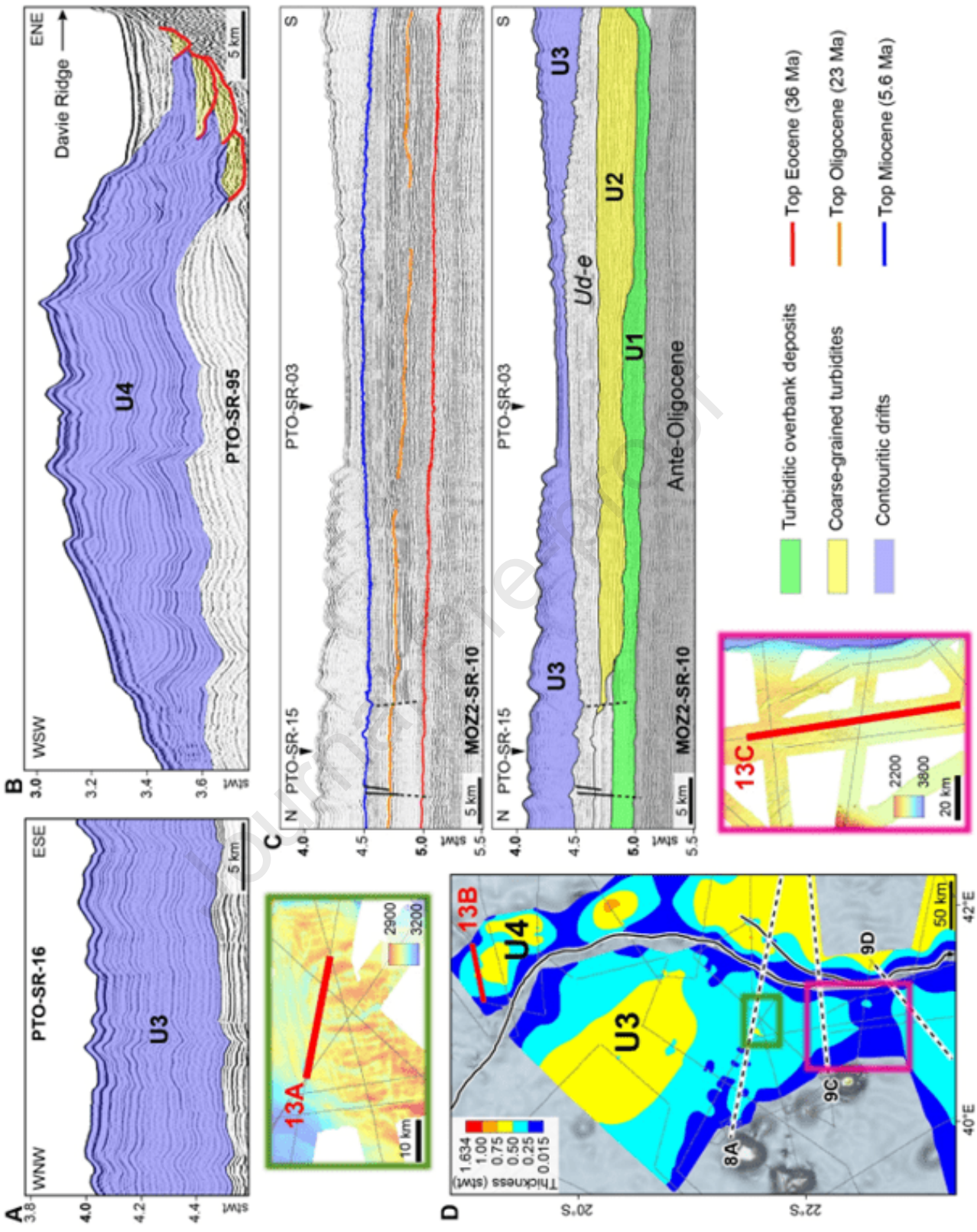

514

515 Figure 13: (A): Detail of unit U3 that is characterized by S1a facies affected by sediment
516 bedforms. (B): Example of contouritic sedimentation near the Davie Ridge as part of unit U4
517 that shows similar shape and internal configuration. (C): A second example of unit U3 more
518 to the south, where it is locally less developed. (D): Zoom of the distribution and isochore

519 map of unit U3 (right hand-side of the Zambezi Valley, see Fig. 10C) and unit U4 (left hand-
520 side of the Zambezi Valley, see Fig. 10D) showing the location of the seismic profiles.
521 Enlarged bathymetric insets show the location of A and C.
522
523 ***Unit U4: Turbidite and contourite deposition on the eastern side of the Zambezi Valley***
524 The left bank (looking downstream) of the Zambezi Valley and both flanks of the Tsiribihina
525 Valley are mainly composed of stratified facies with very continuous medium-amplitude and
526 high-frequency reflections (Fig. 8A, 9). This facies shows truncated reflectors towards the
527 Zambezi Valley and a convergent internal configuration away from the valley axis (Fig 8A,
528 14A), similar to well-known levees of channel-levee systems (e.g. Congo, Amazon, Indus,
529 Mississippi). We therefore interpret this facies as fine-grained overbank turbidites (probably
530 alternating with very fine hemipelagic deposits). The stacking of these turbidites resulted in a
531 ca. 0.7 stwt (~700 m) thick seismic unit (up to 0.9 stwt, ~900 m, locally) (Fig. 10D). Smaller
532 units of inferred coarse-grained turbiditic (Uf, see Fig. 9 and section hereafter) and MTD (Ug,
533 see Fig. 9 and section hereafter) origin are intercalated locally within U4. In addition, towards
534 the east, lateral change in facies and external configuration to wavy parallel reflections (Figs.
535 8A, 14B) suggest a possible contemporaneous contouritic sedimentation on the Madagascar
536 slope and along the Davie Ridge (Fig. 13B). This transition is arbitrary since there is probably
537 a complete gradation between turbiditic and contouritic deposits.
538

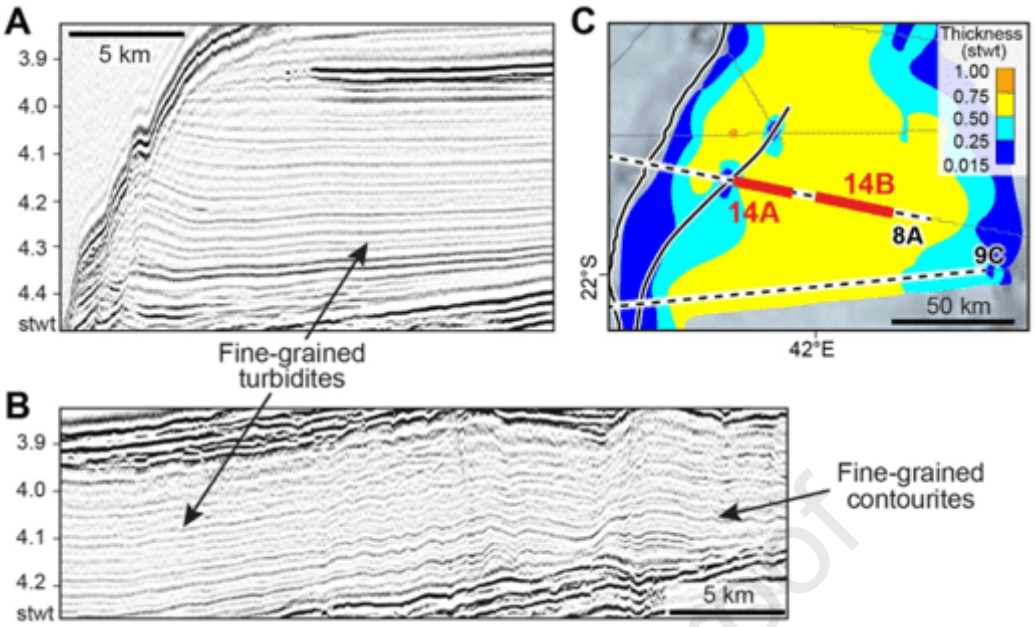

Figure 14: Close up of unit U4 that characterizes the left (looking downstream) border of the Zambezi Valley. (A): Detail on fine-grained turbidites close to the Zambezi Valley, with truncated reflectors towards the valley and convergent internal configuration away from the valley axis. (B): More distally from the valley, a lateral change in facies to a wavy configuration suggests mixed turbidite-contourite deposits. (C): Zoom of the distribution and isochore map of unit U4 with the location of seismic profiles A and B.

Unit U5: Ponded turbidites confined in the Intermediate Basin

Unit U5 is wedge-shaped (Fig. 15) and consists in two main depocenters up to 1.6 stwt (~1600 m) thick (Fig. 10E) along the Mozambique base of slope. It shows numerous small incisions inside it evoking erosional channels and is composed of seismic sub-units that migrate alternately to the NE and SW (Fig. 16D) indicating shifts of depocenters over time. The main core of unit U5, between the Mozambique slope and the Iles Eparses, is composed of an alternation of high-amplitude facies (probably coarse-grained turbidites) and more transparent or even chaotic levels (respectively small but recurrent MTDs and erosional channels) that suggest a cyclic sedimentation (Fig. 16). The base of U5 shows large irregular undulations (erosional structures?) (Figs. 15, 16A) where contourites (possibly related to the

Neogene drift proposed by Raisson et al., 2016) are suspected to be affected by structural doming (Fig. 8).

In its distal most part, between the Iles Eparses and the Zambezi Valley (Fig. 8A), unit U5 appears as an infilling unit composed of continuous, strong amplitude and low frequency reflections with onlapping terminations (facies S2, Figs. 6, 8A) on the supposed contourite drift (Fig. 17).

In the center part of the Intermediate Basin near the Iles Eparses, a transparent cover rests unconformably on the turbiditic deposits (Figs. 16). On sub-bottom profiles, this cover reveals continuous, high frequency reflections with increasing amplitude towards the top (Fig. 16C). These characteristics at the top of the cover suggest an increase in coarse-grained material in the youngest strata. This cover has a variable thickness (ca. 0-100 m) and a limited distribution area. Owing to these characteristics, we suggest that this cover consists of an alternation of contourites or fine-grained turbidites with hemipelagic sediments. Any firm attribution of this superficial cover would need ground truthing by coring.

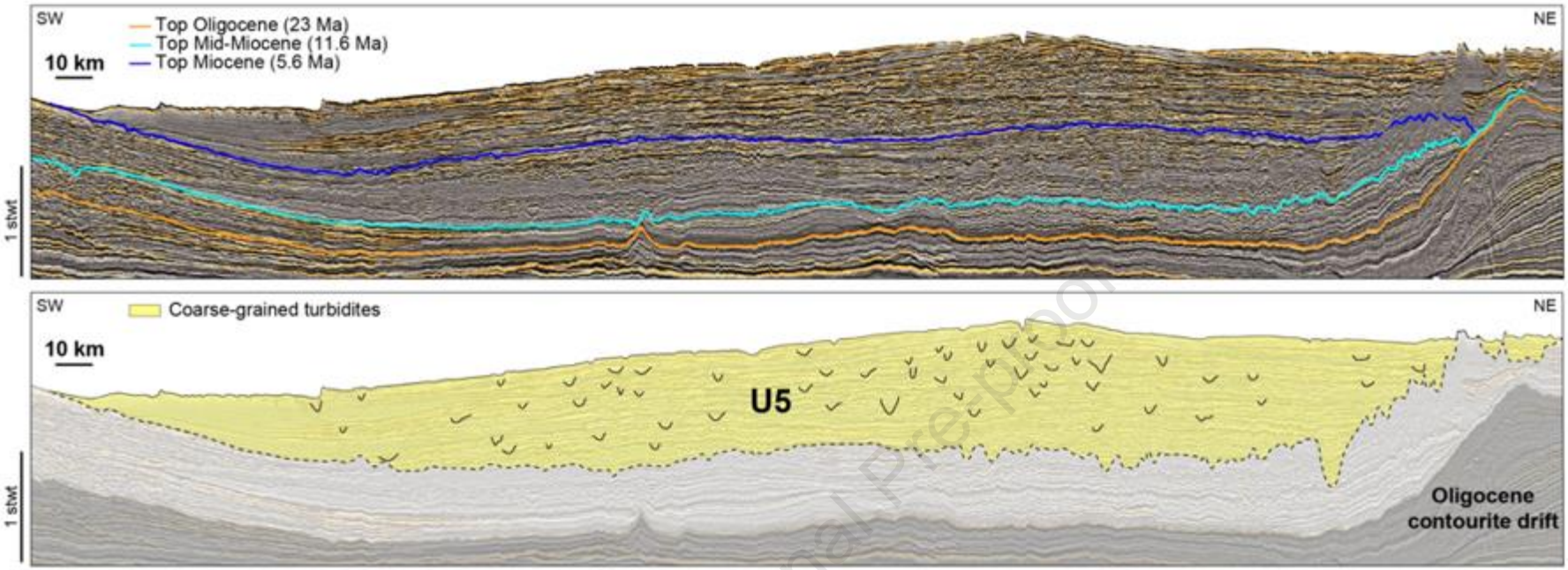

574

575 Figure 15: The architecture of the Ponded Fan. (A) NW-SE seismic section with stratigraphy established by Ponte (2018) and (B) corresponding line
576 drawing with indication of facies, crossing the Intermediate Basin (modified from Thiéblemont et al., 2020, data image courtesy of INP and
577 WesternGeco). The Ponded Fan (infilled by mainly coarse-grained turbidites) is cut by several small incisions (black V forms in B). The position of the
578 profile is shown in Fig. 10E.

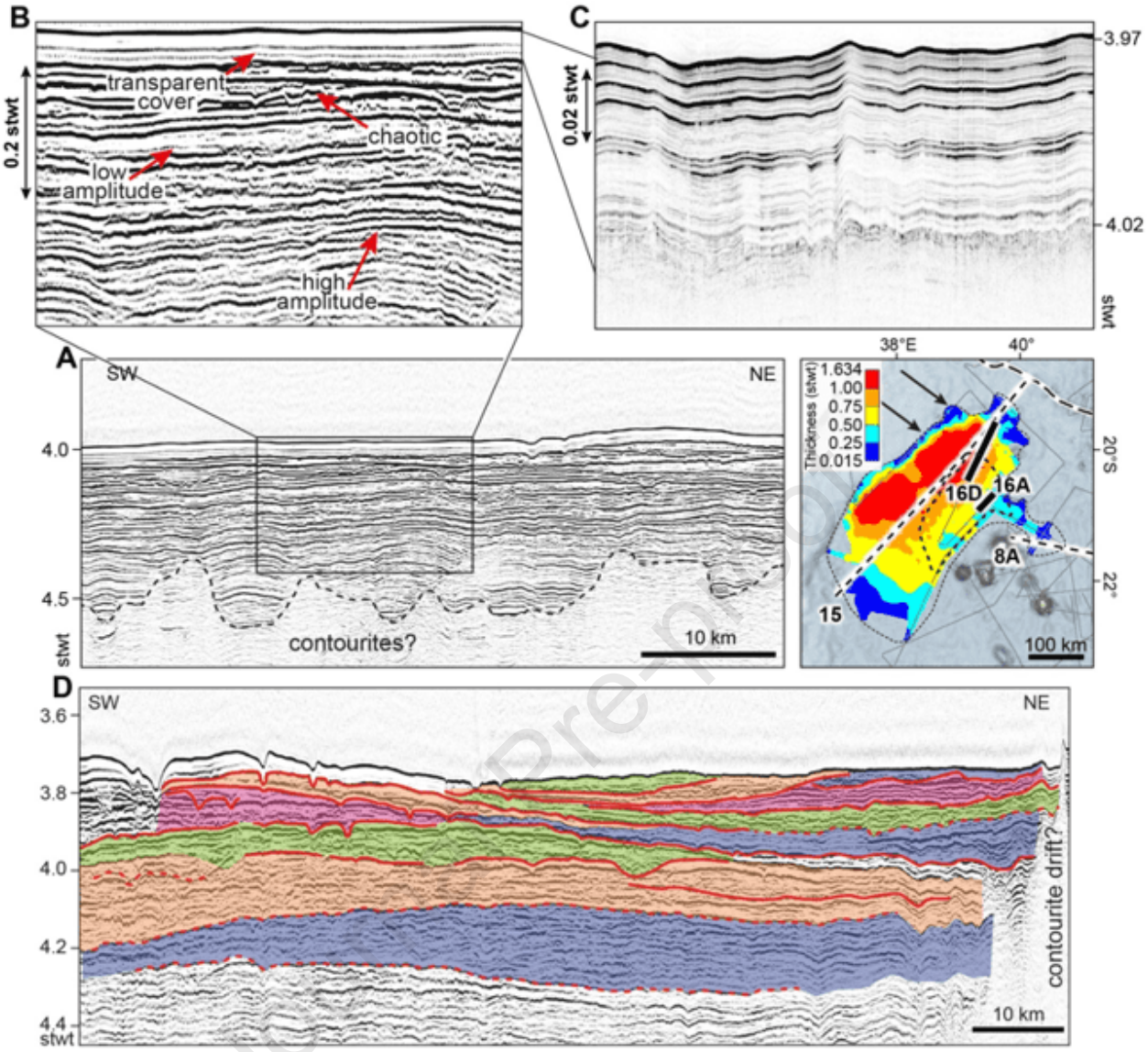

Figure 16: Detail of unit U5 that characterizes the infill of the Intermediate Basin. (A): High-resolution multichannel seismic profile (MOZ4-SR-173) showing the continuous, strong amplitude reflections with low frequency alternating with transparent and chaotic facies. The base of the U5 is delineated by a dashed line. (B): Zoom of A that shows more in detail the vertical variations in amplitude. (C): Transparent cover on a sub-bottom profile (MOZ4-SDS-173d and e with alternating highly stratified facies in uppermost section). (D): Migrations of the depocenters characterizing the filling of the Intermediate Basin (line MOZ4-SR-171a and b). Colors are only used to highlight shifts in seismic units (no particular lithological significance). Note also the decrease in the thickness of the transparent surface layer, until it disappears towards the NE. At its NE limit U5 is onlapping on a contourite drift (Raisson et

590 al., 2016). The location of the seismic profiles A and D is illustrated with a zoom of the
591 distribution and isochore map of unit U5 (See Fig. 10).

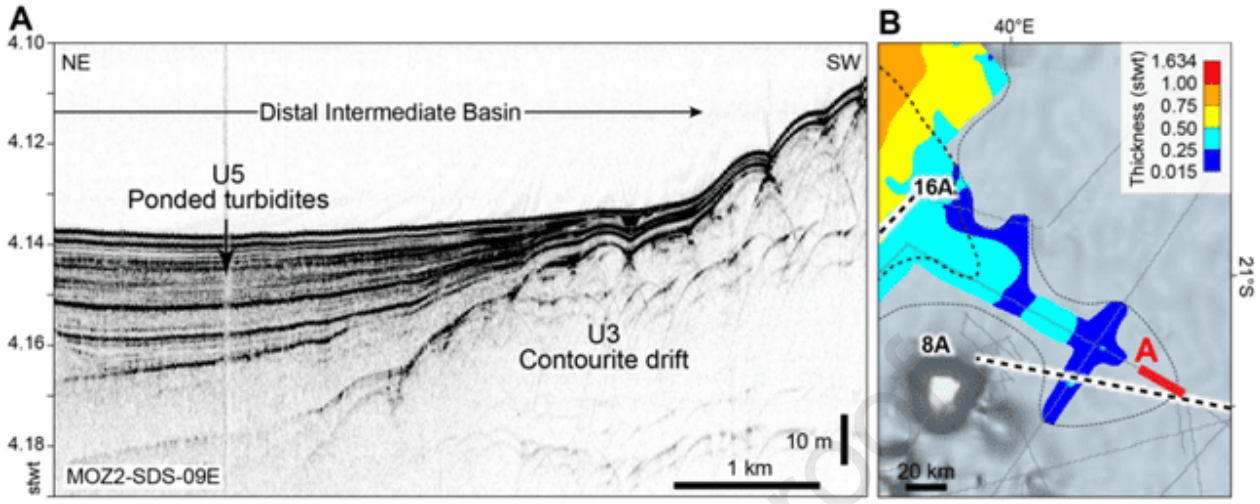

592

593 Figure 17: The distal end of unit U5 (Ponded Fan). (A): Sub-bottom profile illustrating the
594 onlapping terminations on unit U3 (modified from Fierens et al., 2020). (B): Zoom of the
595 distribution and isochore map of unit U5 (see Fig. 10E) showing the location of the sub-
596 bottom profile A.

597

598 4.2.4 Stratigraphy of the seismic units

599 The regional stratigraphic framework of the Mozambique Channel and Zambezi turbidite
600 system (Fig. 4) established by Ponte (2018) allowed us to assign ages for the deposition of
601 seismic units (Fig. 8). Units U1 and U2 were deposited during the Oligocene (between Top
602 Eocene and Top Oligocene horizons) and Early Miocene (between Top Oligocene and Top
603 Mid-Miocene horizon) respectively. Units U3 to U5 are Plio-Quaternary in age (deposited
604 above the Top Miocene horizon). Because of the lack of stratigraphic information on both
605 sides of the valley and because units U3 and U4 are separated by the deeply incised
606 Zambezi Valley, the precise timing of deposition of these units and the stratigraphic
607 continuity of their sedimentary successions are unknown (synchronous or alternative,
608 continuous or discontinuous deposition?). Unit 5 corresponds in profile A of Fig. 8 to the
609 distal part of the Ponded Fan. The main depocenter of U5 is developed updip of the Iles
610 Eparses. Downdip the islands, unit U5 onlaps on unit U3 and appears to have been

deposited late (Late Quaternary?). According to this stratigraphic framework, the Miocene interval and especially the Late Miocene are very thin (only some hundreds of meters in Fig. 8A).

In the distal depositional area (DA), the timing of deposition is different from upstream: turbidite facies are absent during the Oligocene and only began to deposit during the Miocene. It must also be noticed also that contrarily to upstream, the Miocene deposits (especially the Late Miocene) are much thicker.

4.2.4. The Zambezi Valley incisions

While the Oligocene, the Early Miocene and the Plio-Quaternary periods were dominantly characterized by thick aggrading deposits, the Late Miocene period is distinguished by a limited turbiditic deposition (Fig. 8A) and a deep entrenchment of the valley.

The Zambezi Valley is currently deeply incised with relief exceeding 700 m in the middle portion of the valley (Fierens et al., 2019). It evolved during the Miocene through several phases of incision and infilling (Figs. 18, 19), some of them observed continuously all along the Zambezi Valley. Three main incisions, namely Angoche2 (A2), Zambezi1 (Z1) and Zambezi2 (Z2) from the oldest to the youngest (Figs. 9, 18, 19) are identified. Additionally, a fourth incision (Zambezi3, Z3) corresponds to very recent erosion, well expressed on bathymetric data of the valley floor (Fierens et al., 2019). Besides some local shifts that may be observed (e.g., profile 7, Fig. 18 and profile 13, Fig. 19), A2, Z1 and Z2 occur mostly vertically under the current Zambezi Valley, indicating that this valley did not undergo major migration since its formation. Multiple additional minor erosional unconformities inside the valley and in the depositional area (purple unconformities in Fig. 19) are observed but cannot be followed from upstream to downstream.

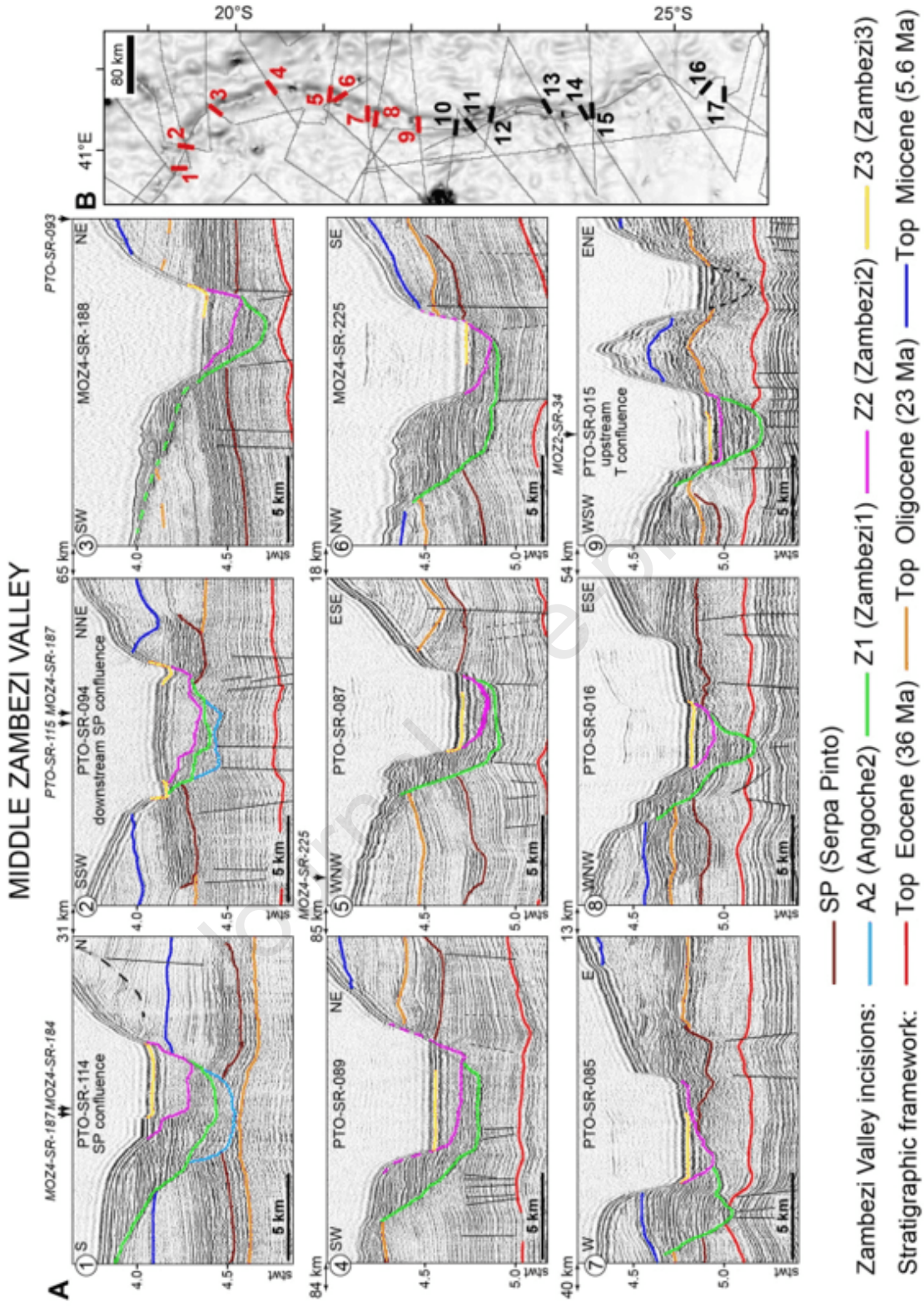

Figures 18: Upstream-downstream evolution of the incisions in the Zambezi Valley upstream of the confluence with the Tsiribihina Valley. Serie of seismic profiles (A): located as red lines on the Gebco slope map (B). Vertical black lines and black arrows in A are faults and profile crossings, respectively. The incision of the Tsiribihina Valley (not studied in this paper) is

640 drawn as a black dashed line in profile 9. Uninterpreted seismic profiles are provided as

641 supplementary material B-1.

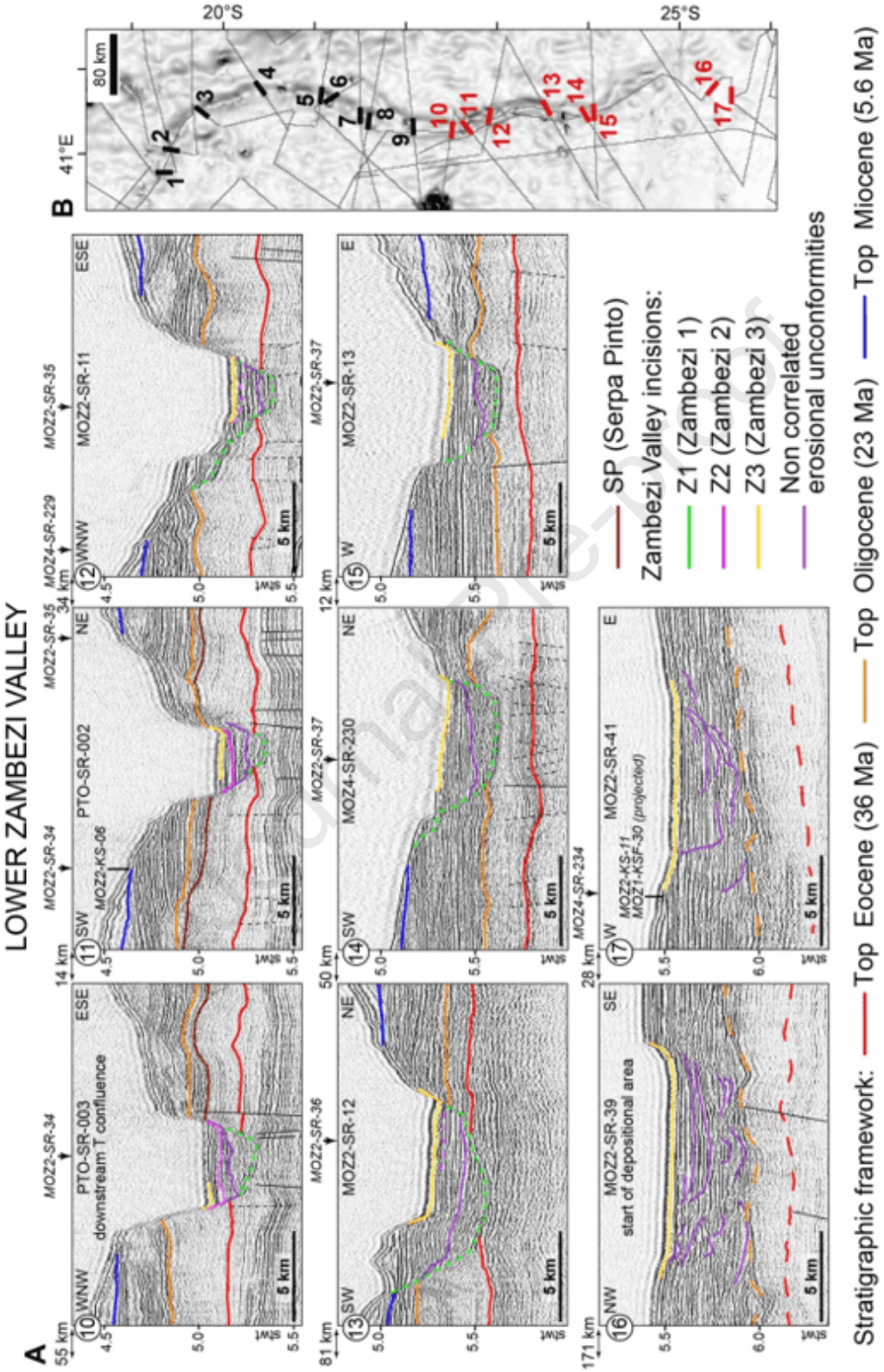

642

643 Figure 19: Upstream-downstream evolution of the incisions in the Zambezi Valley

644 downstream of the confluence with the Tsiribihina Valley. Serie of seismic profiles (A) located

as red lines on the Gebco slope map (B). Vertical black lines and black arrows in A are faults and profile crossings, respectively. Uninterpreted seismic profiles are provided as supplementary material B-2.

A2: Beginning of over-deepening of the Zambezi Valley

Incision A2 is the deepest incision observed on available seismic data. It is recognized only in the upstream portion of the Zambezi Valley, not far upstream from the Angoche Valley-Zambezi Valley confluence (Fig. 18 profile 1). A2 is therefore thought to relate to the Angoche Valley. This incision disappears rapidly downstream because of its erosion by the following incision Z1 (Fig. 18).

As proposed above, the Angoche Valley may have contributed to the feeding of the fan simultaneously with the Serpa Pinto Valley during an initial stage of activity (Angoche1, Fig. 9A). A2 is the trace of the latest incision by the Angoche Valley, when the Serpa Pinto Valley was no longer active. It implies that the Angoche Valley probably deeply incised during its second stage of activity, resulting in the total disappearance of the previous A1 erosional course (Fig. 18, profile 1, 2).

Z1: Main incision resulting in the first occurrence of the upstream part of the Zambezi Valley

Incision Z1 is identified upstream from the Angoche Valley confluence. Consequently, it is considered to indicate the first occurrence of the valley that funneled the inputs of the Zambezi River. It marks the definitive installation of the valley at its present-day position on the central Mozambique margin.

Z1 eroded down to the upper strata of the Eocene sequence (Fig. 18). It is identified all along the Zambezi Valley (Figs. 18, 19). The depth below the current valley floor evolves irregularly from up to ~0.4 stwt (profiles 1 and 8, Fig. 18) to down to ~0.2 stwt (profile 6, Fig. 18), and the depth below sea level varies from 4.4 stwt (profile 1, Fig. 18) to 5.6 stwt on profile 15 (Fig. 19) where it is tentatively identified.

673 Its infill is very thick (more than 0.4 stwt, ~400 m, on profiles 4 to 6, Fig. 18) and is generally
674 made of high-amplitude stratified facies indicating coarse-grained material, with facies that
675 vary on profiles from chaotic to transparent to stratified (Fig. 18, 19).
676
677 ***Z2 and Z3: later incisions of the Zambezi Valley***
678 Incision Z2 is the last main incision of the Zambezi Valley. Its infill is characterized by a 0.2
679 stwt (~200 m) thick transparent body, identified continuously from the upper reaches of the
680 valley to about 100 km southwards of the Tsiribihina confluence. This transparent mass is
681 interpreted as a mass transport deposit (MTD). Above the MTD, a thin layer (at the seismic
682 scale) of sediments is observed, mostly in the upstream portion of the valley.
683 Erosion Z3 is observed all along the Zambezi Valley and represents the youngest erosional
684 events. Compared to previous incision events, this erosive period appears rather negligible.
685 It resulted in local over-deepening of the valley floor up to 0.063 stwt (~63 m) (profiles 1-2,
686 Fig. 18) and gave the valley its current morphology (see Fierens et al., 2019).
687

688 **5. DISCUSSION**

689 **5.1. Origin of depositional units**

690 ***U1: Serpa Pinto channel-levee complex with possible first stage of Angoche Valley***
691 As mentioned previously (Section 4.2.3) unit U1 deposits are related to the Serpa Pinto
692 Valley. The Serpa Pinto Valley received inputs from the northern part of Mozambique (Lurio
693 and probably other northeastern African drainage basins, Ponte, 2018), indicating a 1100 km
694 long transfer of sediments downstream to the most distal area where the channel-levee
695 complex is identified with certainty (Figs. 9E, 10A). Moreover, in the northernmost part of the
696 study area (Fig. 9A), overbank deposition is observed from both the Serpa Pinto and the
697 Angoche Valley. This indicates that there was possibly a contemporaneous first stage of
698 Angoche Valley (Angoche1, Fig. 9) that contributed to the channel-levee complex.

699 The U1 channel-levee complex, which was deposited during the Oligocene, is coeval to the
700 building of the Zambezi giant 1.8 stwt-thick contourite drift on the southern bank of the upper
701 Zambezi Valley (Fig 1B, 20A) (Raisson et al., 2016; Ponte, 2018; Thiéblemont et al., 2020).
702 The juxtaposition of 2 major sedimentation mechanisms raises the question of their possible
703 interaction. It is probable that the dramatic increase in terrigenous sedimentation brought into
704 the basin by valleys (Ponte, 2018), associated with the major modification of global oceanic
705 circulation (Ponte, 2018; Thiéblemont et al., 2020) controls the construction of the giant drift.
706 It is noticeable that the giant drift builds approximately where the northeastward flowing deep
707 waters were interpreted to turn back to the South (Thiéblemont et al., 2020).
708
709

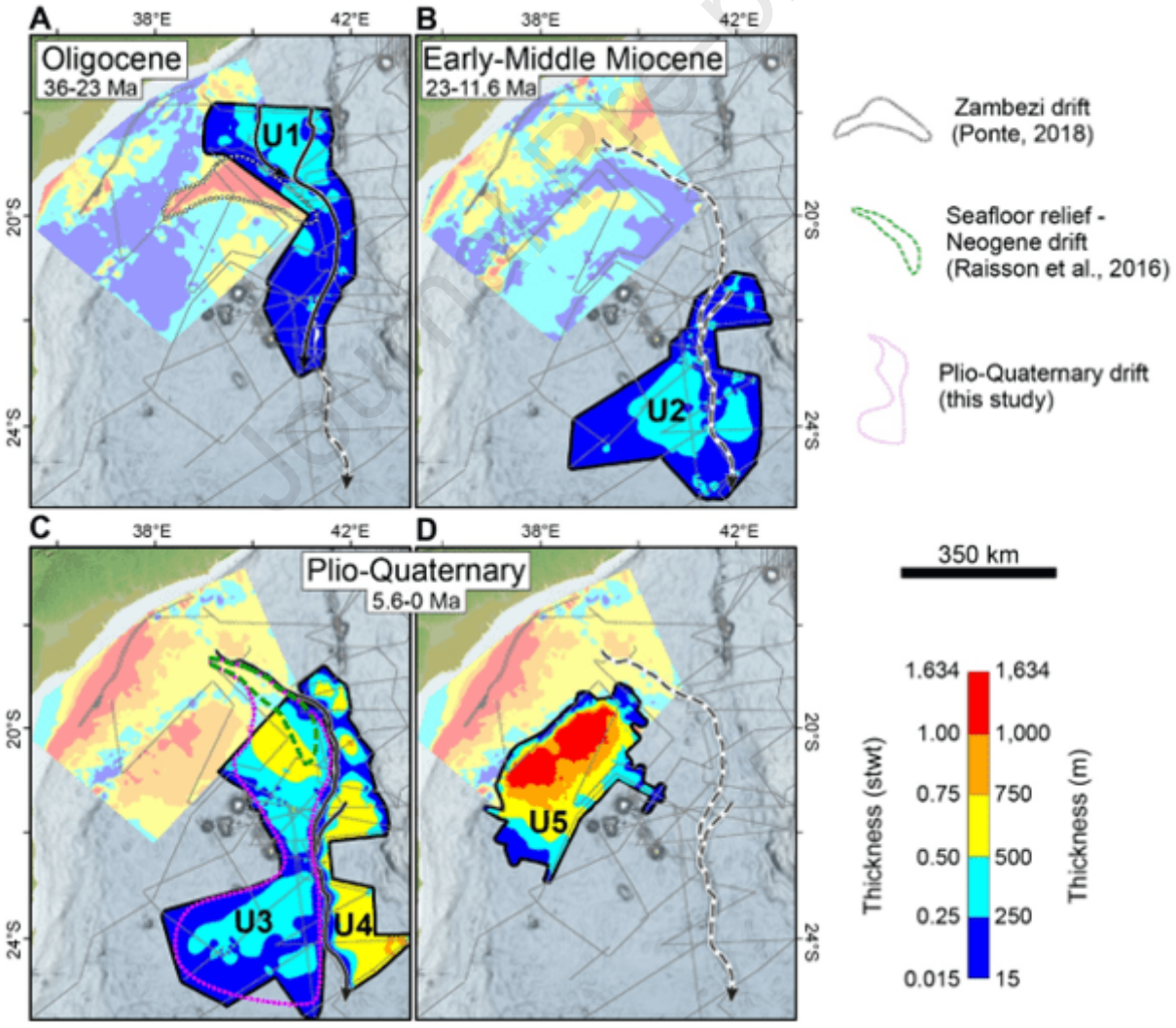

710

Figure 20: Composite thickness maps including the Zambezi turbidite system (this study) (surrounded with a black line) and the upper Mozambique margin (Ponte, 2018). The different contouritic drifts identified are indicated: (A): Oligocene sediment thickness (36-23 Ma); (B): Early-Middle Miocene sediment thickness (23-11.6 Ma); (C) and (D): Plio-Quaternary sediment thickness (5.6 Ma-0 Ma). See Fig. 10 for key to understand of black arrowed lines.

U2: Serpa Pinto (or Madagascar) Lobe complex

With the available data, it was not possible to define the upstream extension of unit U2 and therefore the origin of unit U2 could not be properly established. The NE-SW orientation of U2 deposits suggests two possible origins: from the Madagascar margin (paleo-Tsiribihina Valley) or from the Serpa Pinto Valley (with or without the Angoche Valley). However, Delaunay (2018) stated that the overspill of Madagascar inputs to the Zambezi system occurred only from Middle Miocene, when the Morondova Basin was infilled and detrital sediments from Madagascar could overcome the Davie Ridge. The hypothesis of a Madagascan origin of unit U2 appears therefore less convenient and thus a persistent feeding by the Serpa Pinto Valley (or by the combined Serpa Pinto + Angoche valleys) is favored.

U3-U4: Mixed contouritic-turbiditic sedimentation

Units U3 and U4 have been described separately because we do not have any stratigraphic information to give a relative chronology. However, owing to the top Miocene horizon of Ponte (2018), they were both deposited during the Plio-Quaternary, and we think that they were probably contemporaneous.

Unit U3, identified as a contourite drift at a water depth of ca. 2800 to 3500 m, may have been generated by bottom currents associated to the northward flowing Mozambique Undercurrent, which contain the North Atlantic Deep Water (NADW) at this particular depth range (van Aken et al., 2004). This interpretation is consistent with the observation of Miramontes et al. (2019) that the present-day NADW partly flows inside the Zambezi Valley

738 and contribute to the flank erosion and over-widening of the valley. This large contourite drift
739 which developed on the southern bank of the upper Zambezi Valley, just where it bends from
740 a NW-SE to N-S trend (pink dotted polygon in Fig. 20C), is shifted to the SE with regard to
741 the giant Oligocene drift (Fig 20A) and extends more to the SW. The Plio-Quaternary
742 contouritic drift is associated to a sea floor relief (green polygon in Fig 20C) that was formerly
743 called Neogene drift by Raisson et al. (2016). Here again we can suppose that the drift
744 benefited from the terrigenous supply of turbidity current overflows (by possible sediment
745 pirating) whose origin is not clear (as it can come from turbidity currents from the Zambezi
746 Valley and/or distal sediment upwelling to the north).
747 On the left border of the Zambezi Valley and both sides of the Tsiribihina Valley fine-grained
748 levee turbidites dominate (Fig. 8A, 9B-C). The U4 deposit thus indicates that there is a
749 synchronicity of different terrigenous input sources coming from the Mozambique and
750 Madagascar margins. Moreover, the lenticular units Uf and Ug (present in the upper part of
751 unit U4) attest to recurrent inputs from Madagascar that are not funneled into the Tsiribihina
752 Valley. In addition, contourites appear to have been constantly deposited, either
753 synchronously or in alternation with levee deposition, especially in areas approaching high
754 reliefs, such as the Davie Ridge (Fig. 13B).

755 ***U5: Ponded turbidites from the Mozambique slope***

756 The mainly coarse-grained turbidites were fed to the Intermediate Basin through a network of
757 parallel valleys originating from the Mozambique slope off the Zambezi River mouth (Fig.
758 7A). Several channels have been identified, however the density of channels on the slope is
759 rather small (ca. 50 km between each main channel). These valleys disappear halfway up
760 the slope in agreement with the absence of canyons on the highest part of the slope (Jouet
761 and Deville, 2015), demonstrating that there is no current connection between the shelf and
762 the basin (as it was also observed for the Zambezi Valley). Wiles et al. (2017b) showed that
763 channels in the southwestern portion of the basin (see Fig. 1B) probably transfer some of the
764 Zambezi inputs towards the Bourcart-Hall Depression southeast of the Iles Eparses.

765 Based on the stratigraphy of Ponte (2018), the Intermediate Basin began to fill in during the
766 Upper Miocene, while deposition had mainly ceased in the Zambezi Fan that was mainly
767 subject to erosion inside the valley (see Section 5.2), except in the distal depositional area.
768 This is the only period of time during which data highlight a clear absence of synchronicity
769 between both turbidite accumulation sites of the Mozambique margin. Later on, during the
770 Plio-Quaternary, the Intermediate Basin was filled in and sediment deposition happened in
771 the Zambezi Fan.
772 The thickness map (Fig. 10E) is consistent with that of Thiéblemont et al. (2020) (Fig. 20D).
773

774 **5.2. Upstream-downstream evolution of the incisions and effects of the Miocene**
775 **doming**
776

777 The depth profiles of incisions A2 to Z2 (Fig. 21B) show that A2 and Z1 incisions suffered a
778 post-depositional deformation. This deformation is well expressed by the depth profiles of
779 Top Eocene and Top Oligocene horizons observed between km 100 and km 900. It was
780 described by Ponte (2018) as an episode of doming during the Miocene (Fig. 21C).
781

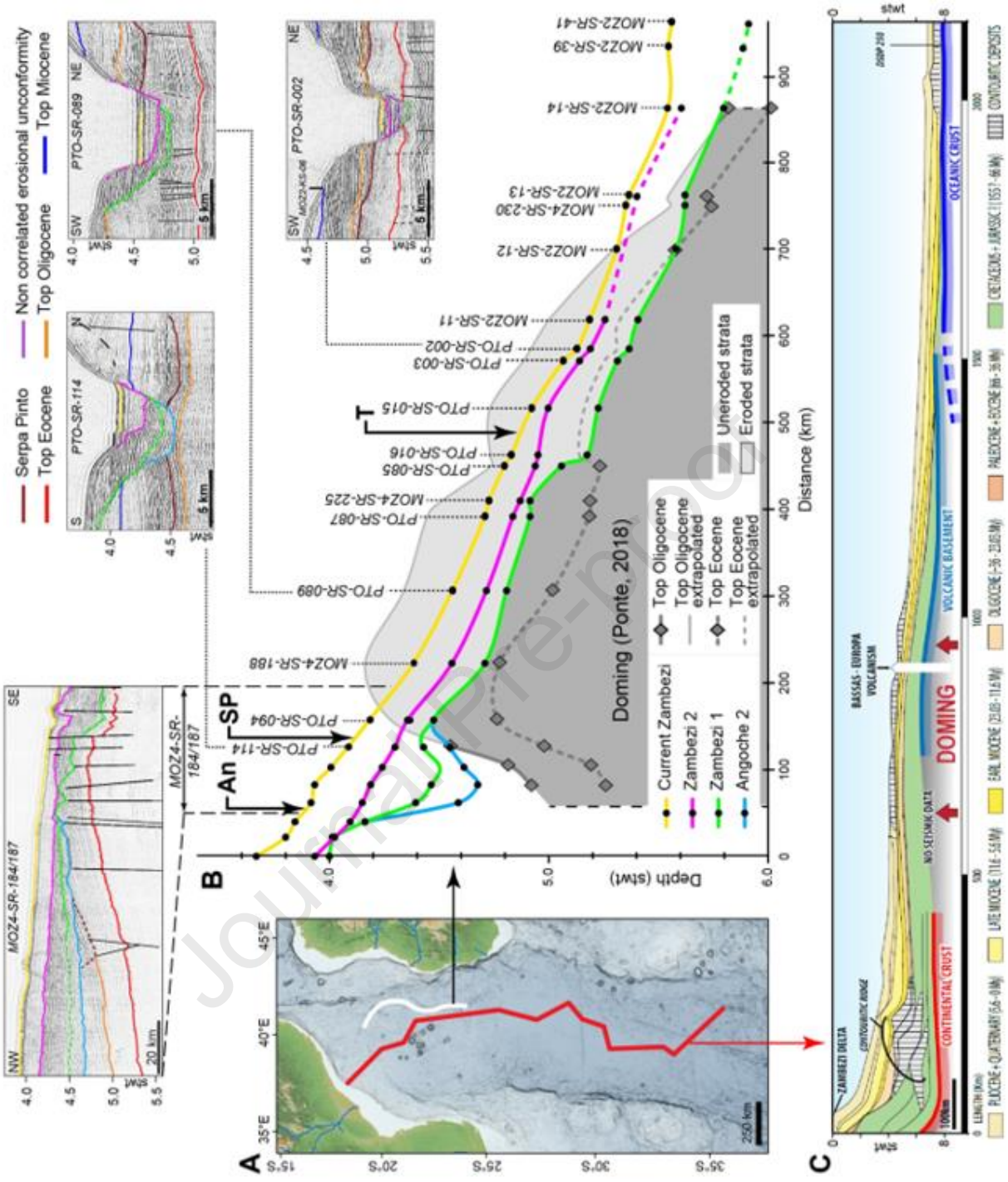

782

783 Figure 21: Effects of the Miocene doming in the central Mozambique Channel on the
784 Zambezi Valley incisions. (A) Position of profiles shown in B (white line) and C (red line). (B)
785 Depth profiles (in stwt) of the main incisions. An, SP and T: Angoche, Serpa Pinto and
786 Tsiribihina confluences, respectively. The depth profiles of the Top Eocene and Top
787 Oligocene horizons are reconstructed from Ponte (2018). (C) Synthetic dip profile of the
788 Mozambique Channel showing the Miocene doming (Ponte, 2018).

The deformation of A2 and Z1 incision profiles (MOZ4-SR-184/187 in Fig. 21B from around 50 to 150 km) and of the Top Eocene and Top Oligocene horizons indicate that the deformation began after the initial incision of A2 and Z1 axes and was prolonged during their activity. This allows dating the A2 and Z1 incisions before the start of the doming deformation in Middle Miocene (Ponte, 2018). On the other hand, we also observe locally the preservation of the Top Oligocene reflector below the A2 incision (see profile PTO-SR-114 on Figs. 18 and 21), so A2 and Z1 are also post-Top Oligocene. The following Z2 and Z3 incisions are not affected by the deformation and have depth profiles close to an equilibrium state. The incision of Z2 happened therefore after the end of doming deformation in Late Miocene according to Ponte (2018).

The continuous deformation resulted in a constant adjustment of the Z1 incision depth profile by entrenchment in order to compensate the uplift movement and to establish a new equilibrium state. The deep entrenchment of Z1 incision resulted in the erosion and disappearance of A2 (and probably also A1). The Z1 depth profile is not at an equilibrium state, it is assumed that it was abandoned prematurely before it had time to reestablish a full equilibrium profile.

The structural deformation on the Zambezi Valley during the Miocene had significant influence on the capacity to transfer sediments downstream. The continuous erosion in link with the elevation of the seafloor during the Miocene resulted in an over-incision of the Z1 incision, the production of important volumes of reworked sediments and the absence of levee deposits related to over-deepening of the valley floor.

The lacking, eroded Oligocene strata are estimated to a minimum of 0.4 stwt thickness (~400 m) and occur at least along 700 km (from profile PTO-SR-094 to profile MOZ2-SR-13, Fig. 21B). If the shape of the Z1 incision is approximated by a half rectangular prism of ca. 700 km long, 400 m high and 4 km wide (mean wideness of Zambezi1 incision, see Fig.18), a rough minimum volume of 560 km^3 of eroded sediments is estimated. This reworked

sedimentary volume is probably deposited downstream. At the time the incision occurred, it was unrelated to input by the Zambezi and other feeding rivers and therefore should be taken into consideration for the erosion-sedimentation balance calculations in source to sink studies. Conversely, the upstream portion of the Z1 incision (Fig. 21B, from km 50 to 150) shows a concave upward-shape suggesting that it could have served as a trap for the Zambezi River inputs. This would have decreased the sedimentary volume able to reach the deeper portions of the Zambezi Fan. However, it can be assumed that the volume of trapped sediments inside Z1 is negligible with regards to the eroded Oligocene strata volumes (from km 150 to km 850, Fig. 21B).

5.3. Distinct modifications in the Zambezi turbidite system development

The Zambezi turbidite system experienced drastic modifications of sediment deposition during its evolution. Since Oligocene, sediment feeding axes migrated westward for the upstream portion of the Zambezi Valley (from SP-A1 to A2 to Z1-Z3) and a general southward migration of deposits happened. This was partly accompanied by successive variations in sedimentological regimes alternating between mainly aggradational and erosional phases (Fig. 22).

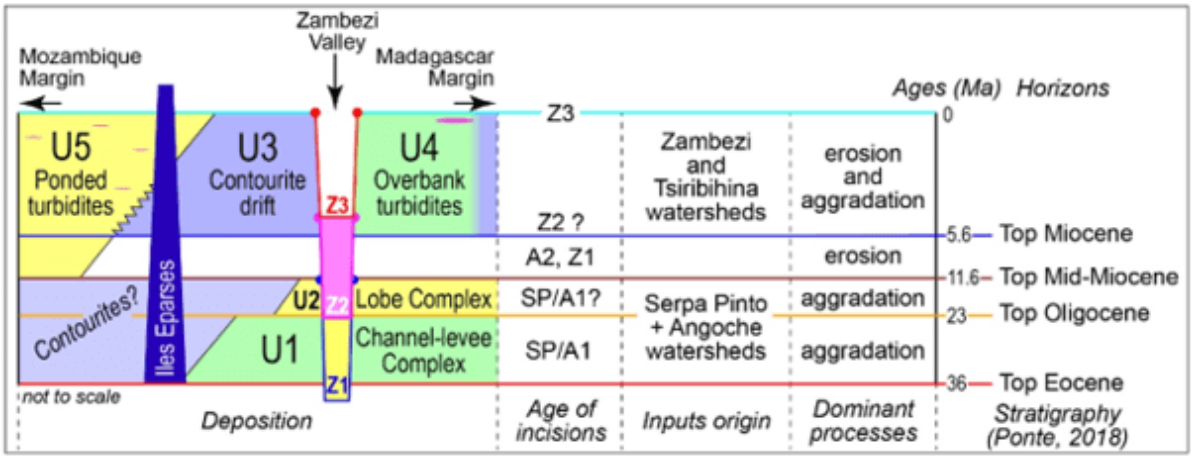

Figure 22: West-east schematic illustration of the timing of seismic unit deposition and main incisions for the Zambezi turbidite system based on the stratigraphy established by Ponte

(2018). Green: fine-grained turbidites; Yellow: coarse-grained turbidites; Blue: contouritic deposition; Pink: mass-transport deposit.

The Oligocene was dominated by mainly fine-grained deposits and aggradational processes with the deposition of the Serpa Pinto channel-levee complex (U1). Limited erosional processes were restricted to the basal surface of the channel and it was possibly combined with a first stage of Angoche Valley activity (Fig. 9A). The deposition evolved during Early Miocene into coarse-grained sediments that are interpreted as distal turbiditic channel-mouth deposits of the Serpa Pinto system (U2). Their installation on previous more proximal channel-levees could reflect the retrogradation of the system. The origin of the change in depositional regime and possible retrogradation is unknown, but is probably related to the offshore tectonic deformation in the eastern branch of the East African Rift (Courgeon et al., 2018), which would provoke changes in sediment flux supplied from North Mozambique.
The thickness map of Miocene sediments (Fig. 20B) shows that deposition started in the Intermediate Basin, while the Zambezi Fan is dominated by erosional processes during Middle to Late Miocene. This with two successive incisions (A2 and Z1) that indicate a shift of the position of the source, from the Angoche to the Zambezi drainage basin. In the Late Miocene, the incisions were affected by a progressive structural doming in the central part of the Mozambique Channel (Ponte, 2018). Oligocene strata were eroded and the Angoche2 incision was probably totally erased by the Z1 erosional phase in response to the long-lasting elevation of the seafloor during Late Miocene. This incision period must have produced an important volume of material (estimated to 560 km^3, see section 5.2) that is probably deposited downstream in the Depositional Area. It was however not possible to individualize the seismic units associated to this episode of strong erosion.
Later on in the Late Miocene a new aggradational stage happened were the Z1 incision was infilled with onlapping sediments probably in order to establish a new equilibrium profile and deposition started in the Intermediate Basin.

The Plio-Pleistocene is characterized by a combination of aggradational and erosional events that resulted in a diversification of deposits. Fine-grained turbidites are observed at the left overbank of the Zambezi Fan, while mainly coarse-grained turbidites are present in the Intermediate Basin and Depositional Area. Contourites occur on the right bank of the Zambezi Valley as well as in the Angoche basin. Additionally, this period is characterized by synchronicity of different terrigenous input sources (Zambezi and Madagascar margin). The Zambezi Valley (incision Z2; Figs. 18, 19) is in a rather equilibrium state. It was lately infilled by a MTD, observed 800 km along the Zambezi Valley more downstream than the Tsiribihina confluence (Fig. 18, 19 profiles 1-11). Considering the maximum thickness of this MTD (0.2 stwt, ~200 m), the mean wideness of the Z2 incision (4 km), and a rectangular prism as an approximation of the shape of the MTD, a rough estimation of the volume of transported sediments can be calculated to 640 km^3. Together with the MTDs in the distal Depositional Area, the occurrence of these mass transport deposits attests to the recurrence of instabilities in the Plio-Pleistocene period, also shown on the Mozambique slope by Ponte (2018).

The Zambezi Fan has been shown to be dominantly erosional during very recent times (Fierens et al., 2019; Miramontes et al., 2019). The erosional regime is attested by multiple generations of incisions in the thalweg (corresponding to the Z3 incision), erosion of the valley flanks possibly by bottom currents, and absence (or rarity) of fine-grained deposits (pirating of the turbulent suspension cloud by contouritic currents?). Contrarily, in the Ponded Fan, the depositional regime is mainly aggradational.

6. CONCLUSION

Academic high-resolution seismic data complemented with industrial data allowed deciphering the Oligocene to present architectural evolution of the Zambezi turbidite system including the Zambezi channelized Fan and the Intermediate Ponded Fan. Seismic interpretation allowed distinguishing five major depositional units and four principal incisional

episodes. The respective depositional timing of these units is established based on the regional stratigraphy from Ponte (2018).

The main results can be summarized as follows:

- The Zambezi turbidite system is shown to be composed of both turbidites and contourites that were deposited mostly synchronously along the Mozambique and Madagascar margins. The history of the turbidite system shows an alternation of aggradational and erosional processes.
- Stratigraphic correlations place the Serpa Pinto (and Angoche1) deposition (unit U1) during the Oligocene, the distal turbiditic deposition (unit U2) during Early Miocene, the Angoche2 and Zambezi1 incisions during Middle - Late Miocene and the Zambezi2 incision at the beginning of the Pliocene. Units U3 and U4 were deposited during the Plio-Quaternary.
- Succession of valleys that fed the sedimentary units evidences an anticlockwise shift of feeding axes from the Serpa Pinto Valley to the Angoche Valley and finally towards the Zambezi Valley. This goes together with a shift of the drainage basins that fed the fan, from the northern most watersheds of the Mozambique (Lurio and possible other northern rivers) to the Angoche watershed (more south), then to the Zambezi watershed (central Mozambique).
- The main incision event occurred during the Late Miocene, when the valley suffered the effects of a structural doming in the central part of the Mozambique Channel. The continuous elevation of the seafloor forced the profound entrenchment of the Zambezi1 incision (~400 m of erosion), which supposedly is cause of the observed absence of lateral levees proximal to the Zambezi Valley. Products of this strong erosional regime (estimated to 560 km^3 of reworked sediments) are supposed to be transported to the distal Depositional Area.
- Most turbiditic deposits in the studied area are either fine-grained levee turbidites (units U1 and U4) or coarse-grained channel-mouth turbidites (U2, U5 and Depositional Area).

- Mass-movement processes, recurrent on the Mozambique slope (Ponte, 2018) since the Pliocene have been observed mainly in the Zambezi Valley, in the distal depositional area, and on the Madagascar margin.
- Contouritic sedimentation is at least continuous since the Oligocene. The drift sediments are supposed to be supplied by turbiditic processes (current overflow) and both (i.e. turbiditic and contouritic) depositional processes occur most often synchronous (i.e. U3 during U4 levee deposition, possibly during northern Serpa Pinto deposition and close to the Davie Ridge). Besides the two thickest Oligocene and Miocene drifts upstream on the margin, a prominent Plio-Quaternary N-S contourite drift (U3) is identified on the right flank of the Zambezi Valley where bottom current controlled bedforms are observed.

This study has important implications for the current understanding of deep-marine turbidite systems. It demonstrates the sensitivity of large depositional systems to changing basin floor topography created by progressive structural deformation in terms of the architectural elements and the associated capacity to transfer sediments downstream.

ACKNOWLEDGEMENTS

The PhD thesis of Ruth Fierens was co-funded by TOTAL and IFREMER as part of the PAMELA (Passive Margin Exploration Laboratories) scientific project. The PAMELA project is a scientific project led by Ifremer and TOTAL in collaboration with Université de Bretagne Occidentale, Université Rennes 1, Université Pierre and Marie Curie, CNRS and IFP-EN. We thank the Captains and crew members of the 2014 and 2015 cruises PTOLEMEE and PAMELA-MOZ2 onboard the R/V L'Atalante and PAMELA-MOZ4 onboard of R/V Pourquoi pas? as well as the technicians from Genavir that ensured acquisitions of the geophysical data. The onboard scientific teams of PAMELA surveys are greatly thanked for their contribution to data acquisitions. Seismic data were analyzed using Kingdom Suite software, kindly made available to UBO by IHS in the framework of their Educational Grant Program. The authors are also grateful to Jacob A. Covault and David Hodgson for their critical reading and constructive

946 discussions at a preliminary stage of this work. We greatly acknowledge the reviews from the
947 Editor in Chief Istvan Csato and from an anonymous reviewer who greatly helped improving
948 the paper.

949

950 **REFERENCES**

951 Adeogba, A.A., McHargue, T.R., Graham, S.A., 2005. Transient fan architecture and
952 depositional controls from near-surface 3-D seismic data, Niger Delta continental slope.
953 AAPG bulletin 89, 627–643. https://doi.org/10.1306/11200404025
954 Alexander, J., Morris, S., 1994. Observations on experimental, nonchannelized, high-
955 concentration turbidity currents and variations in deposits around obstacles. Journal of
956 Sedimentary Research 64, 899–909. https://doi.org/10.1306/D4267F00-2B26-11D7-
957 8648000102C1865D
958 Amante, C., Eakins, B.W., 2009. ETOPO1 arc-minute global relief model: procedures, data
959 sources and analysis. NOAA Technical Memorandum NESDIS NGDC-24, Accessed 25
960 Feb. 2019. https://doi.org/10.7289/V5C8276M
961 Babonneau, N., Savoye, B., Cremer, M., Klein, B., 2002. Morphology and architecture of the
962 present canyon and channel system of the Zaire deep-sea fan. Marine and Petroleum
963 Geology 19, 445–467. https://doi.org/10.1016/S0264-8172(02)00009-0
964 Baby, G., 2017. Mouvements verticaux des marges passives d'Afrique australe depuis 130
965 Ma, étude couplée: stratigraphie de bassin: analyse des formes du relief. Ph.D. Thesis,
966 Université de Rennes 1. France. p. 363.
967 Badhani, S., Cattaneo, A., Dennielou, B., Leroux, E., Colin, F., Thomas, Y., Jouet, G.,
968 Rabineau, M., Droz, L., 2020. Morphology of retrogressive failures in the Eastern Rhone
969 interfluve during the last glacial maximum (Gulf of Lions, Western Mediterranean).
970 Geomorphology 351, 106894. https://doi.org/10.1016/j.geomorph.2019.106894
971 Beaubouef, R.T., Friedmann, S.J., 2000. High Resolution Seismic/Sequence Stratigraphic
972 Framework for the Evolution of Pleistocene Intra Slope Basins, Western Gulf of Mexico:

973 Depositional Models and Reservoir Analogs. Presented at the Deep-water reservoirs of
974 the world: Gulf Coast Section SEPM 20th Annual Research Conference.
975 Beiersdorf, H., Kudrass, H.-R., Stackelberg, U. von, 1980. Placer Deposits of limenite and
976 Zircon on the Zambezi Shelf. Geologisches Jahrbuch Reihe D 500, 36, 1–85.
977 Bourillet, J.-F., Ferry, J.-N., Bourges, P., 2013. PAMELA “PASSIVE MARGINS
978 EXPLORATION LABORATORIES.” http://dx.doi.org/10.18142/236
979 Bozzano, G., Cerredo, M.E., Remesal, M., Steinmann, L., Hanebuth, T.J.J., Schwenk, T.,
980 Baqués, M., Hebbeln, D., Spoltore, D., Silvestri, O., Acevedo, R.D., Spiess, V., Violante,
981 R.A., Kasten, S., 2021. Dropstones in the Mar del Plata Canyon Area (SW Atlantic):
982 Evidence for Provenance, Transport, Distribution, and Oceanographic Implications.
983 Geochem Geophys Geosyst 22. https://doi.org/10.1029/2020GC009333
984 Breitzke, M., Wiles, E., Krocker, R., Watkeys, M.K., Jokat, W., 2017. Seafloor morphology in
985 the Mozambique Channel: evidence for long-term persistent bottom-current flow and
986 deep-reaching eddy activity. Marine Geophysical Research 38, 241–269.
987 https://doi.org/10.1007/s11001-017-9322-7
988 Bursik, M.I., Woods, A.W., 2000. The Effects of Topography on Sedimentation from Particle-
989 Laden Turbulent Density Currents. Journal of Sedimentary Research 70, 53–63.
990 https://doi.org/10.1306/2DC408FE-0E47-11D7-8643000102C1865D
991 Calais, E., Ebinger, C., Hartnady, C., Nocquet, J.M., 2006. Kinematics of the East African Rift
992 from GPS and earthquake slip vector data. Geological Society, London, Special
993 Publications 259, 9–22. https://doi.org/10.1144/GSL.SP.2006.259.01.03
994 Castelino, J.A., Reichert, C., Jokat, W., 2017. Mesozoic and Early Cenozoic sediment influx
995 and morphology of the Mozambique Basin. Marine Geophysical Research.
996 https://doi.org/10.1007/s11001-017-9305-8
997 Clark, I.R., Cartwright, J.A., 2009. Interactions between submarine channel systems and
998 deformation in deepwater fold belts: Examples from the Levant Basin, Eastern
999 Mediterranean sea. Marine and Petroleum Geology 26, 1465–1482.
1000 https://doi.org/10.1016/j.marpetgeo.2009.05.004

1001 Cochran, J.R., 1988. Somali Basin, Chain Ridge, and origin of the Northern Somali Basin
1002 gravity and geoid low. Journal of Geophysical Research: Solid Earth 93, 11985–12008.
1003 https://doi.org/10.1029/JB093iB10p11985
1004 Coffin, M.F., Rabinowitz, P.D., 1987. Reconstruction of Madagascar and Africa: evidence
1005 from the Davie fracture zone and western Somali basin. Journal of Geophysical
1006 Research: Solid Earth 92, 9385–9406. https://doi.org/10.1029/JB092iB09p09385
1007 Counts, J.W., Jorry, S.J., Leroux, E., Miramontes, E., Jouet, G., 2018. Sedimentation
1008 adjacent to atolls and volcano-cored carbonate platforms in the Mozambique Channel
1009 (SW Indian Ocean). Marine Geology 404, 41–59.
1010 https://doi.org/10.1016/j.margeo.2018.07.003
1011 Courgeon, S., Bachèlery, P., Jouet, G., Jorry, S.J., Bou, E., BouDagher-Fadel, M.K.,
1012 Révillon, S., Camoin, G., Poli, E., 2018. The offshore east African rift system: new
1013 insights from the Sakalaves seamounts (Davie Ridge, SW Indian Ocean). Terra Nova
1014 30(5), 380–388.
1015 Courgeon, S., Jorry, S.J., Camoin, G.F., BouDagher-Fadel, M., Jouet, G., Révillon, S.,
1016 Bachèlery, P., Pelleter, E., Borgomano, J., Poli, E., 2016. Growth and demise of
1017 Cenozoic isolated carbonate platforms: New insights from the Mozambique Channel
1018 seamounts (SW Indian Ocean). Marine Geology 380, 90–105.
1019 https://doi.org/10.1016/j.margeo.2016.07.006
1020 Courgeon, S., Jorry, S.J., Jouet, G., Camoin, G., BouDagher-Fadel, M., Bachèlery, P.,
1021 Caline, B., Boichard, R., Révillon, S., Thomas, Y., 2017. Impact of tectonic and volcanism
1022 on the Neogene evolution of isolated carbonate platforms (SW Indian Ocean).
1023 Sedimentary Geology 355, 114–131. https://doi.org/10.1016/j.sedgeo.2017.04.008
1024 Dawson, J.B., 1992. Neogene tectonics and volcanicity in the North Tanzania sector of the
1025 Gregory Rift Valley: contrasts with the Kenya sector. Tectonophysics 204, 81–92.
1026 https://doi.org/10.1016/0040-1951(92)90271-7

1027 Delaunay, A., 2018. Les mouvements verticaux de Madagascar (90-0 Ma): une analyse
1028 couplée des formes du relief et de l'enregistrement sédimentaire des marges ouest
1029 malgaches. Ph.D. Thesis, Université de Rennes 1. France. p. 374.
1030 Dennielou, B., Jégou, I., Droz, L., Jouet, G., Cattaneo, A., Berné, S., Aslanian, D., Loubrieu,
1031 B., Rabineau, M., Bermell, S., 2019. Major modification of sediment routing by a large
1032 Mass Transport Deposit in the Gulf of Lions (Western Mediterranean). Marine Geology
1033 411, 1–20. https://doi.org/10.1016/j.margeo.2019.01.011
1034 Deptuck, M.E., Steffens, G.S., Barton, M., Pirmez, C., 2003. Architecture and evolution of
1035 upper fan channel-belts on the Niger Delta slope and in the Arabian Sea. Marine and
1036 Petroleum Geology 20, 649–676. https://doi.org/10.1016/j.marpetgeo.2003.01.004
1037 Deville, E., Marsset, T., Courgeon, S., Jatiault, R., Ponte, J.-P., Thereau, E., Jouet, G., Jorry,
1038 S.J., Droz, L., 2018. Active fault system across the oceanic lithosphere of the
1039 Mozambique Channel: Implications for the Nubia–Somalia southern plate boundary.
1040 Earth and Planetary Science Letters 502, 210–220.
1041 https://doi.org/10.1016/j.epsl.2018.08.052
1042 Droz, L., Mougenot, D., 1987. Mozambique upper fan: origin of depositional units. AAPG
1043 Bulletin 71, 1355–1365.
1044 Fierens, R., Droz, L., Toucanne, S., Raisson, F., Jouet, G., Babonneau, N., Miramontes, E.,
1045 Landurain, S., Jorry, S.J., 2019. Late Quaternary geomorphology and sedimentary
1046 processes in the Zambezi turbidite system (Mozambique Channel). Geomorphology 334,
1047 1–28. https://doi.org/10.1016/j.geomorph.2019.02.033
1048 Fierens, R., Toucanne, S., Droz, L., Jouet, G., Raisson, F., Jorissen, E.L., Bayon, G.,
1049 Giraudeau, J., Jorry, S.J., 2020. Quaternary sediment dispersal in the Zambezi turbidite
1050 system (SW Indian Ocean). Marine Geology 428, 106276.
1051 https://doi.org/10.1016/j.margeo.2020.106276
1052 Franke, D., Jokat, W., Ladage, S., Stollhofen, H., Klimke, J., Lutz, R., Mahanjane, E.S.,
1053 Ehrhardt, A., Schreckenberger, B., 2015. The offshore East African Rift System:

1054 Structural framework at the toe of a juvenile rift. Tectonics 34, 2086–2104.
1055 https://doi.org/10.1002/2015TC003922
1056 Gaina, C., Van Hinsbergen, D.J., Spakman, W., 2015. Tectonic interactions between India
1057 and Arabia since the Jurassic reconstructed from marine geophysics, ophiolite geology,
1058 and seismic tomography. Tectonics 34, 875–906. https://doi.org/10.1002/2014TC003780
1059 García, M., Hernández-Molina, F.J., Llave, E., Stow, D.A.V., León, R., Fernández-Puga,
1060 M.C., Diaz del Río, V., Somoza, L., 2009. Contourite erosive features caused by the
1061 Mediterranean Outflow Water in the Gulf of Cadiz: Quaternary tectonic and
1062 oceanographic implications. Marine Geology 257, 24–40.
1063 https://doi.org/10.1016/j.margeo.2008.10.009
1064 Garzanti, E., Pastore, G., Resentini, A., Vezzoli, G., Vermeesch, P., Ngube, L., Niekerk, E.V.,
1065 Jouet, G., Dall'Asta, M., in press. The Segmented Zambezi Sedimentary System from
1066 Source to Sink 1. Sand Petrology and Heavy Minerals. The Journal of Geology.
1067 https://doi.org/10.1086/715792
1068 Garziglia, S., Migeon, S., Ducassou, E., Loncke, L., Mascle, J., 2008. Mass-transport
1069 deposits on the Rosetta province (NW Nile deep-sea turbidite system, Egyptian margin):
1070 Characteristics, distribution, and potential causal processes. Marine Geology 250, 180–
1071 198. https://doi.org/10.1016/j.margeo.2008.01.016
1072 GEBCO, 2014. GEBCO_2014 Grid. British Oceanographic Data Centre (BODC). Available
1073 at: http://www.gebco.net/data_and_products/gridded_bathymetry_data/.
1074 Gee, M., Masson, D.G., Watts, A., 2001. Passage of debris flows and turbidity currents
1075 through a topographic constriction: seafloor erosion and deflection of flow pathways.
1076 Gee, M.J.R., Gawthorpe, R.L., 2006. Submarine channels controlled by salt tectonics:
1077 Examples from 3D seismic data offshore Angola. Marine and Petroleum Geology 23,
1078 443–458. https://doi.org/10.1016/j.marpetgeo.2006.01.002
1079 Hall, I.R., Hemming, S.R., LeVay, L.J., Barker, S.R., Berke, M.A., Brentegani, L., Caley, T.,
1080 Cartagena-Sierra, A., Charles, C.D., Coenen, J.J., 2016. International Ocean Discovery

1081 Program; Expedition 361 preliminary report; South African climates (Agulhas LGM density
1082 profile); 30 January-31 March 2016. https://doi.org/10.14379/iodp.pr.361.2016
1083 Haughton, P.D.W., 2000. Evolving turbidite systems on a deforming basin floor, Tabernas,
1084 SE Spain. Sedimentology 47, 497–518. https://doi.org/10.1046/j.1365-3091.2000.00293.x
1085 Hernández-Molina, F.J., Paterlini, M., Somoza, L., Violante, R., Arecco, M.A., de Isasi, M.,
1086 Rebesco, M., Uenzelmann-Neben, G., Neben, S., Marshall, P., 2010. Giant mounded
1087 drifts in the Argentine Continental Margin: Origins, and global implications for the history
1088 of thermohaline circulation. Marine and Petroleum Geology 27, 1508–1530.
1089 https://doi.org/10.1016/j.marpetgeo.2010.04.003
1090 Hodgson, D.M., Haughton, P.D.W., 2004. Impact of syndepositional faulting on gravity
1091 current behaviour and deep-water stratigraphy: Tabernas-Sorbas Basin, SE Spain.
1092 Geological Society, London, Special Publications 222, 135–158.
1093 https://doi.org/10.1144/GSL.SP.2004.222.01.08
1094 Howlett, D.M., Gawthorpe, R.L., Ge, Z., Rotevatn, A., Jackson, C.A.-L., 2020. Turbidites,
1095 topography and tectonics: Evolution of submarine channel-lobe systems in the salt-
1096 influenced Kwanza Basin, offshore Angola. Basin Research n/a.
1097 https://doi.org/10.1111/bre.12506
1098 Hsiung, K.-H., Yu, H.-S., Chiang, C.-S., 2018. The modern Kaoping transient fan offshore
1099 SW Taiwan: Morphotectonics and development. Geomorphology 300, 151–163.
1100 https://doi.org/10.1016/j.geomorph.2017.10.013
1101 Huyghe, P., Foata, M., Deville, E., Mascle, G., Group, C.W., 2004. Channel profiles through
1102 the active thrust front of the southern Barbados prism. Geology 32, 429–432.
1103 https://doi.org/10.1130/G20000.1
1104 Imbo, Y., De Batist, M., Canals, M., Prieto, M.J., Baraza, J., 2003. The Gebra Slide: a
1105 submarine slide on the Trinity Peninsula Margin, Antarctica. Marine Geology 193, 235–
1106 252. https://doi.org/10.1016/S0025-3227(02)00664-3
1107 Janocko, M., Nemec, W., Henriksen, S., Warchoł, M., 2013. The diversity of deep-water
1108 sinuous channel belts and slope valley-fill complexes. Marine and Petroleum Geology,

1109 Special Issue: Internal architecture, bedforms and geometry of turbidite channels 41, 7–
1110 34. https://doi.org/10.1016/j.marpetgeo.2012.06.012
1111 Jorry, S.J., 2014. PTOLEMEE cruise, RV L'Atalante. http://dx.doi.org/10.17600/14000900
1112 Jorry, S.J., Camoin, G.F., Jouet, G., Le Roy, P., Vella, C., Courgeon, S., Prat, S., Fontanier,
1113 C., Paumard, V., Boulle, J., 2016. Modern sediments and Pleistocene reefs from isolated
1114 carbonate platforms (Iles Eparses, SW Indian Ocean): A preliminary study. Acta
1115 Oecologica 72, 129–143. https://doi.org/10.1016/j.actao.2015.10.014
1116 Jouet, G., Deville, E., 2015. PAMELA-MOZ04 cruise, RV Pourquoi Pas ?
1117 http://dx.doi.org/10.17600/15000700
1118 Kolla, V., Eittreim, S., Sullivan, L., Kostecki, J.A., Burckle, L.H., 1980a. Current-controlled,
1119 abyssal microtopography and sedimentation in Mozambique Basin, southwest Indian
1120 Ocean. Marine Geology 34, 171–206. https://doi.org/10.1016/0025-3227(80)90071-7
1121 Kolla, V., Kostecki, J.A., Henderson, L., Hess, L., 1980b. Morphology and Quaternary
1122 sedimentation of the Mozambique Fan and environs, southwestern Indian Oceans.
1123 Sedimentology 27, 357–378. https://doi.org/10.1111/j.1365-3091.1980.tb01188.x
1124 Kukowski, N., Schillhorn, T., Huhn, K., von Rad, U., Husen, S., Flueh, E.R., 2001.
1125 Morphotectonics and mechanics of the central Makran accretionary wedge off Pakistan.
1126 Marine Geology 173, 1–19. https://doi.org/10.1016/S0025-3227(00)00167-5
1127 Le Gall, B., Nonnotte, P., Rolet, J., Benoit, M., Guillou, H., Mousseau-Nonnotte, M., Albaric,
1128 J., Deverchère, J., 2008. Rift propagation at craton margin.: Distribution of faulting and
1129 volcanism in the North Tanzanian Divergence (East Africa) during Neogene times.
1130 Tectonophysics 448, 1–19. https://doi.org/10.1016/j.tecto.2007.11.005
1131 Leinweber, V.T., Jokat, W., 2012. The Jurassic history of the Africa–Antarctica corridor—new
1132 constraints from magnetic data on the conjugate continental margins. Tectonophysics
1133 530, 87–101. https://doi.org/10.1016/j.tecto.2011.11.008
1134 Loncke, L., Gaullier, V., Droz, L., Ducassou, E., Migeon, S., Mascle, J., 2009. Multi-scale
1135 slope instabilities along the Nile deep-sea fan, Egyptian margin: a general overview.

1136 Marine and Petroleum Geology 26, 633–646.
1137 https://doi.org/10.1016/j.marpetgeo.2008.03.010
1138 Lort, J.M., Limond, W.Q., Segoufin, J., Patriat, P., Delteil, J.R., Damotte, B., 1979. New
1139 seismic data in the Mozambique Channel. Marine Geophysical Research 4, 71–89.
1140 Mahanjane, E.S., 2014. The Davie Fracture Zone and adjacent basins in the offshore
1141 Mozambique Margin – A new insights for the hydrocarbon potential. Marine and
1142 Petroleum Geology 57, 561–571. https://doi.org/10.1016/j.marpetgeo.2014.06.015
1143 Mahanjane, E.S., 2012. A geotectonic history of the northern Mozambique Basin including
1144 the Beira High – A contribution for the understanding of its development. Marine and
1145 Petroleum Geology 36, 1–12. https://doi.org/10.1016/j.marpetgeo.2012.05.007
1146 Maselli, V., Kroon, D., Iacopini, D., Wade, B.S., Pearson, P.N., Haas, H. de, 2020. Impact of
1147 the East African Rift System on the routing of the deep-water drainage network offshore
1148 Tanzania, western Indian Ocean. Basin Research 32, 789–803.
1149 https://doi.org/10.1111/bre.12398
1150 Mayall, M., Lonergan, L., Bowman, A., James, S., Mills, K., Primmer, T., Pope, D., Rogers,
1151 L., Skeene, R., 2010. The response of turbidite slope channels to growth-induced seabed
1152 topography. Bulletin 94, 1011–1030. https://doi.org/10.1306/01051009117
1153 Milliman, J.D., Farnsworth, K.L., 2011. River discharge to the coastal ocean: a global
1154 synthesis. Cambridge University Press, p. 392.
1155 Milliman, J.D., Syvitski, J.P., 1992. Geomorphic/tectonic control of sediment discharge to the
1156 ocean: the importance of small mountainous rivers. The Journal of Geology 100, 525–
1157 544. https://doi.org/10.1086/629606
1158 Miramontes, E., 2016. Submarine landslides in the Northern Tyrrhenian Sea and relationship
1159 with the turbiditic and contouritic deposits: morphology, stratigraphy, geotechnics and
1160 modelling. Ph.D. Thesis, Université de Bretagne occidentale, France. p. 215.
1161 Miramontes, E., Penven, P., Fierens, R., Droz, L., Toucanne, S., Jorry, S.J., Jouet, G.,
1162 Pastor, L., Jacinto, R.S., Gaillot, A., 2019. The influence of bottom currents on the
1163 Zambezi Valley morphology (Mozambique Channel, SW Indian Ocean): In situ current

observations and hydrodynamic modelling. Marine Geology 410, 42–55. https://doi.org/10.1016/j.margeo.2019.01.002

Miramontes, E., Thiéblemont, A., Babonneau, N., Penven, P., Raisson, F., Droz, L., Jorry, S.J., Fierens, R., Counts, J.W., Wilckens, H., Cattaneo, A., Jouet, G., 2021. Contourite and mixed turbidite-contourite systems in the Mozambique Channel (SW Indian Ocean): Link between geometry, sediment characteristics and modelled bottom currents. Marine Geology 437, 106502. https://doi.org/10.1016/j.margeo.2021.106502

Mitchum, R.M., Vail, P.R., Sangree, J.B., 1977. Seismic stratigraphy and global changes of sea level: Part 6. Stratigraphic interpretation of seismic reflection patterns in depositional sequences: Section 2. Application of seismic reflection configuration to stratigraphic interpretation. in 'Seismic Stratigraphy–Applications to Hydrocarbon Exploration (C. E. Payton, Ed.)'. 53–62.

Morgan, R., 2004. Structural Controls on the Positioning of Submarine Channels on the Lower Slopes of the Niger Delta. Geological Society, London, Memoirs 29, 45–52. https://doi.org/10.1144/GSL.MEM.2004.029.01.05

Morris, S.A., Alexander, J., 2003. Changes in Flow Direction at a Point Caused by Obstacles During Passage of a Density Current. Journal of Sedimentary Research 73, 621–629. https://doi.org/10.1306/112502730621

Mougenot, D., Recq, M., Virlogeux, P., Lepvrier, C., 1986. Seaward extension of the East African Rift. Nature 321, 599–603. https://doi.org/10.1038/321599a0

Mueller, C.O., Jokat, W., Schreckenberger, B., 2016. The crustal structure of Beira High, central Mozambique—Combined investigation of wide-angle seismic and potential field data. Tectonophysics 683, 233–254. https://doi.org/10.1016/j.tecto.2016.06.028

Mutti, E., Normark, W.R., 1991. An Integrated Approach to the Study of Turbidite Systems, in: Weimer, P., Link, M.H. (Eds.), Seismic Facies and Sedimentary Processes of Submarine Fans and Turbidite Systems, Frontiers in Sedimentary Geology. Springer New York, New York, NY, pp. 75–106. https://doi.org/10.1007/978-1-4684-8276-8_4

1191 Mutti, E., Normark, W.R., 1987. Comparing examples of modern and ancient turbidite
1192 systems: problems and concepts, in: Marine Clastic Sedimentology. Springer, pp. 1–38.
1193 Nugent, C., 1990. The Zambezi River: tectonism, climatic change and drainage evolution.
1194 Palaeogeography, Palaeoclimatology, Palaeoecology 78, 55–69.
1195 https://doi.org/10.1016/0031-0182(90)90204-K
1196 Oluboyo, A.P., Gawthorpe, R.L., Bakke, K., Hadler-Jacobsen, F., 2014. Salt tectonic controls
1197 on deep-water turbidite depositional systems: Miocene, southwestern Lower Congo
1198 Basin, offshore Angola. Basin Research 26, 597–620. https://doi.org/10.1111/bre.12051
1199 Piper, Hiscott, Normark, 1999. Outcrop-scale acoustic facies analysis and latest Quaternary
1200 development of Hueneme and Dume submarine fans, offshore California. Sedimentology
1201 46, 47–78. https://doi.org/10.1046/j.1365-3091.1999.00203.x
1202 Ponte, J.-P., 2018. La marge africaine du canal du Mozambique (le système turbiditique du
1203 Zambèze) : une approche « Source to Sink » au Méso - Cénozoïque. Ph.D. Thesis,
1204 Université de Rennes 1. France. p. 351.
1205 Ponte, J.-P., Robin, C., Guillocheau, F., Popescu, S., Suc, J.-P., Dall'Asta, M., Melinte-
1206 Dobrinescu, M.C., Bubik, M., Dupont, G., Gaillot, J., 2019. The Zambezi delta
1207 (Mozambique channel, East Africa): High resolution dating combining bio- orbital and
1208 seismic stratigraphies to determine climate (palaeoprecipitation) and tectonic controls on
1209 a passive margin. Marine and Petroleum Geology 105, 293–312.
1210 https://doi.org/10.1016/j.marpetgeo.2018.07.017
1211 Rabinowitz, P.D., Coffin, M.F., Falvey, D., 1983. The Separation of Madagascar and Africa.
1212 Science 220, 67–69. https://doi.org/10.1126/science.220.4592.67
1213 Raisson, F., Cazzola, C., Ferry, J.-N., 2016. Deep oceanic currents and sea floor interactions
1214 offshore SE Africa. Presented at the EGU General Assembly Conference Abstracts, 18,
1215 Vienna (Austria), p. 18459.
1216 Reading, H.G., 1991. The classification of deep-sea depositional systems by sediment
1217 caliber and feeder system. Journal of the Geological Society 148, 427–430.
1218 https://doi.org/10.1144/gsjgs.148.3.0427

1219 Reading, H.G., Richards, M., 1994. Turbidite systems in deep-water basin margins classified
1220 by grain size and feeder system. AAPG bulletin 78, 792–822.
1221 Reeves, C., 2014. The position of Madagascar within Gondwana and its movements during
1222 Gondwana dispersal. Journal of African Earth Sciences, Geology and metallogeny of the
1223 Precambrian basement of Madagascar 94, 45–57.
1224 https://doi.org/10.1016/j.jafrearsci.2013.07.011
1225 Reichert, C., Aslanian, D., 2007. MD 163 / MOBAMASIS cruise,Marion Dufresne R/V.
1226 https://doi.org/10.17600/7200110
1227 Robin, C., Droz, L., 2014. PAMELA-MOZ02 cruise, RV L'Atalante.
1228 http://dx.doi.org/10.17600/14001100
1229 Roquette, E., 2016. La marge transformante nord-Mozambicaine : bilan érosion -
1230 sédimentation. (Technical report). Université de Rennes 1.
1231 Rowan, M.G., Weimer, P., 1998. Salt-Sediment Interaction, Northern Green Canyon and
1232 Ewing Bank (Offshore Louisiana), Northern Gulf of Mexico. AAPG Bulletin 82, 1055–
1233 1082.
1234 Saller, A.H., Noah, J.T., Ruzuar, A.P., Schneider, R., 2004. Linked lowstand delta to basin-
1235 floor fan deposition, offshore Indonesia: An analog for deep-water reservoir systems.
1236 AAPG Bulletin 88, 21–46. https://doi.org/10.1306/09030303003
1237 Salman, G., Abdula, I., 1995. Development of the Mozambique and Ruvuma sedimentary
1238 basins, offshore Mozambique. Sedimentary Geology 96, 7–41.
1239 https://doi.org/10.1016/0037-0738(95)00125-R
1240 Saria, E., Calais, E., Stamps, D.S., Delvaux, D., Hartnady, C.J.H., 2014. Present-day
1241 kinematics of the East African Rift. Journal of Geophysical Research: Solid Earth 119,
1242 3584–3600. https://doi.org/10.1002/2013JB010901
1243 Schulz, H., Lückge, A., Emeis, K.-C., Mackensen, A., 2011. Variability of Holocene to Late
1244 Pleistocene Zambezi riverine sedimentation at the upper continental slope off
1245 Mozambique, 15°–21°S. Marine Geology 286, 21–34.
1246 https://doi.org/10.1016/j.margeo.2011.05.003

1247 Segoufin, J., Patriat, P., 1981. Reconstructions de l'Ocean Indien Occidental pour les
1248 epoques des anomalies M21, M2 et 34; Paleoposition de Madagascar. Bulletin de la
1249 Société géologique de France 7, 603–607. https://doi.org/10.2113/gssgfbull.S7-
1250 XXIII.6.603
1251 Simpson, E.S.W., 1974. Sites 243 and 244. Vol. 25, 177–186.
1252 https://doi.org/10.2973/dsdp.proc.25.106.1974
1253 Sinclair, H.D., Tomasso, M., 2002. Depositional evolution of confined turbidite basins.
1254 Journal of Sedimentary Research 72, 451–456.
1255 Smith, R., 2004. Silled sub-basins to connected tortuous corridors: sediment distribution
1256 systems on topographically complex sub-aqueous slopes. Geological Society, London,
1257 Special Publications 222, 23–43. https://doi.org/10.1144/GSL.SP.2004.222.01.03
1258 Stamps, D.S., Iaffaldano, G., Calais, E., 2015. Role of mantle flow in Nubia-Somalia plate
1259 divergence. Geophysical Research Letters 42, 290–296.
1260 https://doi.org/10.1002/2014GL062515
1261 Stow, D.A.V., Howell, D.G., Nelson, C.H., 1985. Sedimentary, Tectonic, and Sea-Level
1262 Controls, in: Bouma, A.H., Normark, W.R., Barnes, N.E. (Eds.), Submarine Fans and
1263 Related Turbidite Systems, Frontiers in Sedimentary Geology. Springer, New York, NY,
1264 pp. 15–22. https://doi.org/10.1007/978-1-4612-5114-9_4
1265 Thiéblemont, A., Hernández-Molina, F.J., Ponte, J.-P., Robin, C., Guillocheau, F., Cazzola,
1266 C., Raisson, F., 2020. Seismic stratigraphic framework and depositional history for
1267 Cretaceous and Cenozoic contourite depositional systems of the Mozambique Channel,
1268 SW Indian Ocean. Marine Geology 106192.
1269 https://doi.org/10.1016/j.margeo.2020.106192
1270 Thomas, D.S., Shaw, P.A., 1988. Late Cainozoic drainage evolution in the Zambezi Basin:
1271 geomorphological evidence from the Kalahari rim. Journal of African Earth Sciences (and
1272 the Middle East) 7, 611–618. https://doi.org/10.1016/0899-5362(88)90111-X

1273 Thompson, J.O., 2017. The opening of the Indian Ocean: what is the impact on the East
1274 African, Madagascar and Antartictic margins, and what are the origins if the aseismic
1275 ridges? Ph.D. Thesis, Université de Rennes 1, France. p. 189.
1276 Thompson, J.O., Moulin, M., Aslanian, D., de Clarens, P., Guillocheau, F., 2019. New
1277 starting point for the Indian Ocean: Second phase of breakup for Gondwana. Earth-
1278 Science Reviews 191, 26–56. https://doi.org/10.1016/j.earscirev.2019.01.018
1279 van Aken, H.M., Ridderinkhof, H., de Ruijter, W.P., 2004. North Atlantic deep water in the
1280 south-western Indian Ocean. Deep Sea Research Part I: Oceanographic Research
1281 Papers 51, 755–776. https://doi.org/10.1016/j.dsr.2004.01.008
1282 Van Rooij, D., Iglesias, J., Hernández-Molina, F.J., Ercilla, G., Gomez-Ballesteros, M.,
1283 Casas, D., Llave, E., De Hauwere, A., Garcia-Gil, S., Acosta, J., Henriet, J.-P., 2010. The
1284 Le Danois Contourite Depositional System: Interactions between the Mediterranean
1285 Outflow Water and the upper Cantabrian slope (North Iberian margin). Marine Geology
1286 274, 1–20. https://doi.org/10.1016/j.margeo.2010.03.001
1287 Walford, H., White, N., Sydow, J., 2005. Solid sediment load history of the Zambezi Delta.
1288 Earth and Planetary Science Letters 238, 49–63.
1289 https://doi.org/10.1016/j.epsl.2005.07.014
1290 Wiles, E., Green, A., Watkeys, M., Jokat, W., 2017a. The Zambezi Channel: A new
1291 perspective on submarine channel evolution at low latitudes. Geomorphology 286, 121–
1292 132. https://doi.org/10.1016/j.geomorph.2017.02.014
1293 Wiles, E., Green, A.N., Watkeys, M.K., Jokat, W., 2017b. Zambezi continental margin:
1294 compartmentalized sediment transfer routes to the abyssal Mozambique Channel. Marine
1295 Geophysical Research 1–14. https://doi.org/10.1007/s11001-016-9301-4
1296 Wiles, E., Watkeys, M., Jokat, W., 2020. Surface expression of microplate boundary
1297 kinematics: An isolated abyssal hill in the Mozambique Channel. Journal of African Earth
1298 Sciences 168, 103830. https://doi.org/10.1016/j.jafrearsci.2020.103830

1299 Winker, C.D., 1996. High-resolution seismic stratigraphy of a late Pleistocene submarine fan
1300 ponded by salt-withdrawal mini-basins on the Gulf of Mexico continental slope. Presented
1301 at the Offshore Technology Conference, Offshore Technology Conference, pp. 619–628.
1302 Zindorf, M., Rooze, J., Meile, C., März, C., Jouet, G., Newton, R., Brandily, C., Pastor, L.,
1303 2021. The evolution of early diagenetic processes at the Mozambique margin during the
1304 last glacial-interglacial transition. Geochimica et Cosmochimica Acta 300, 79–94.
1305 https://doi.org/10.1016/j.gca.2021.02.024
1306
1307

Supplementary material A

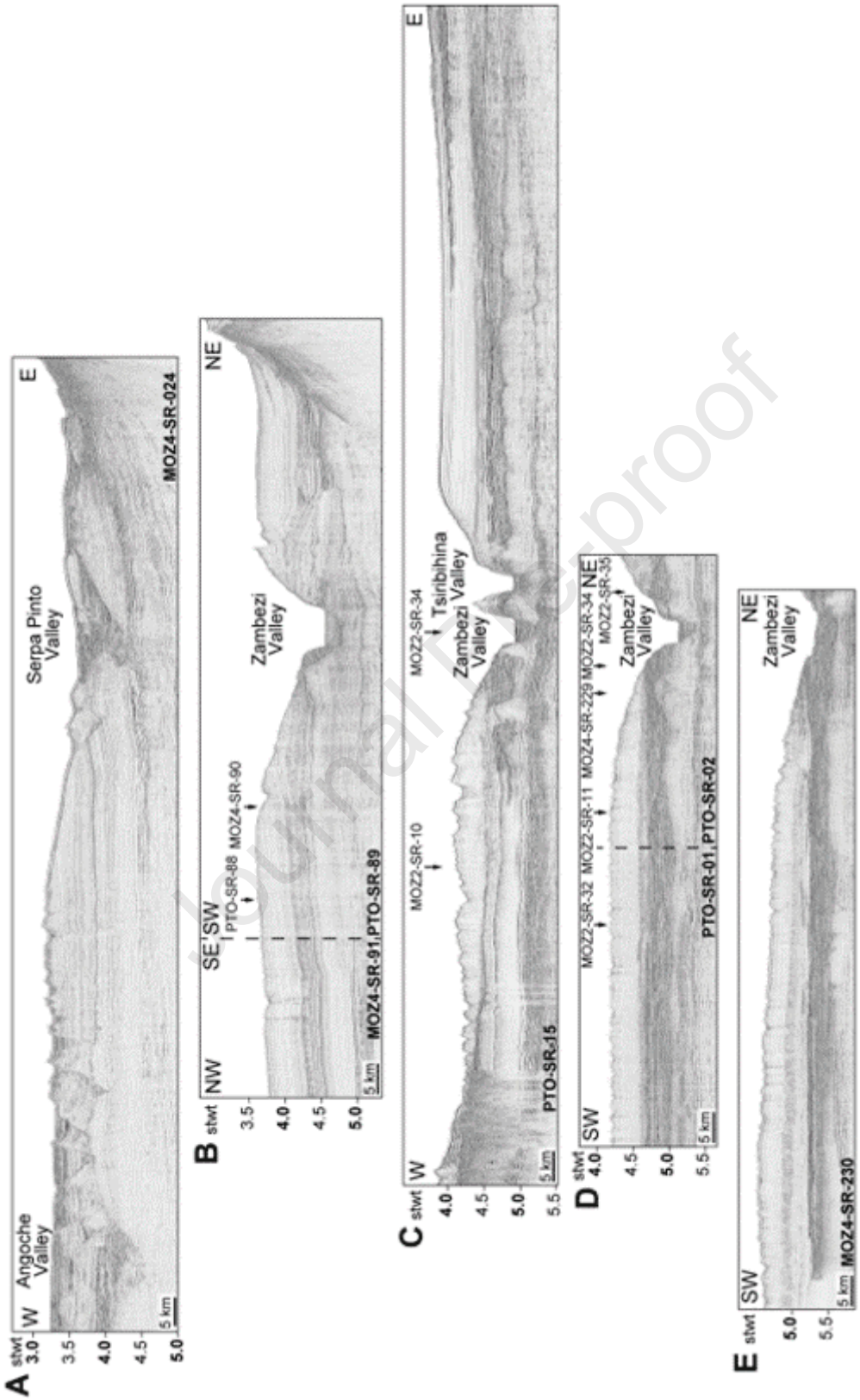

Supplementary material A: Uninterpreted profiles of figure 9.

Supplementary material B-1

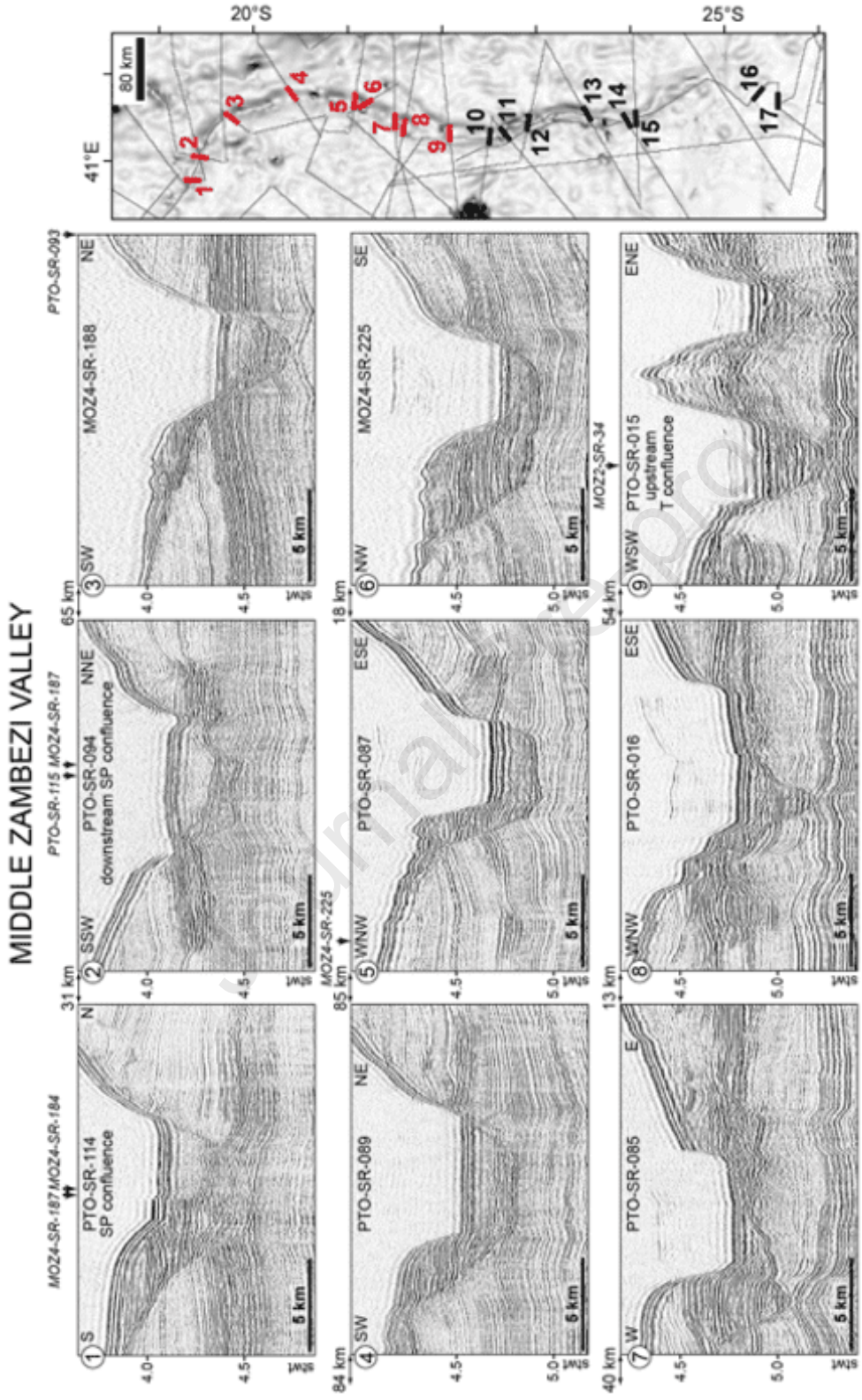

Supplementary material B-1: Uninterpreted seismic profiles of figure 18.

Supplementary material B-2

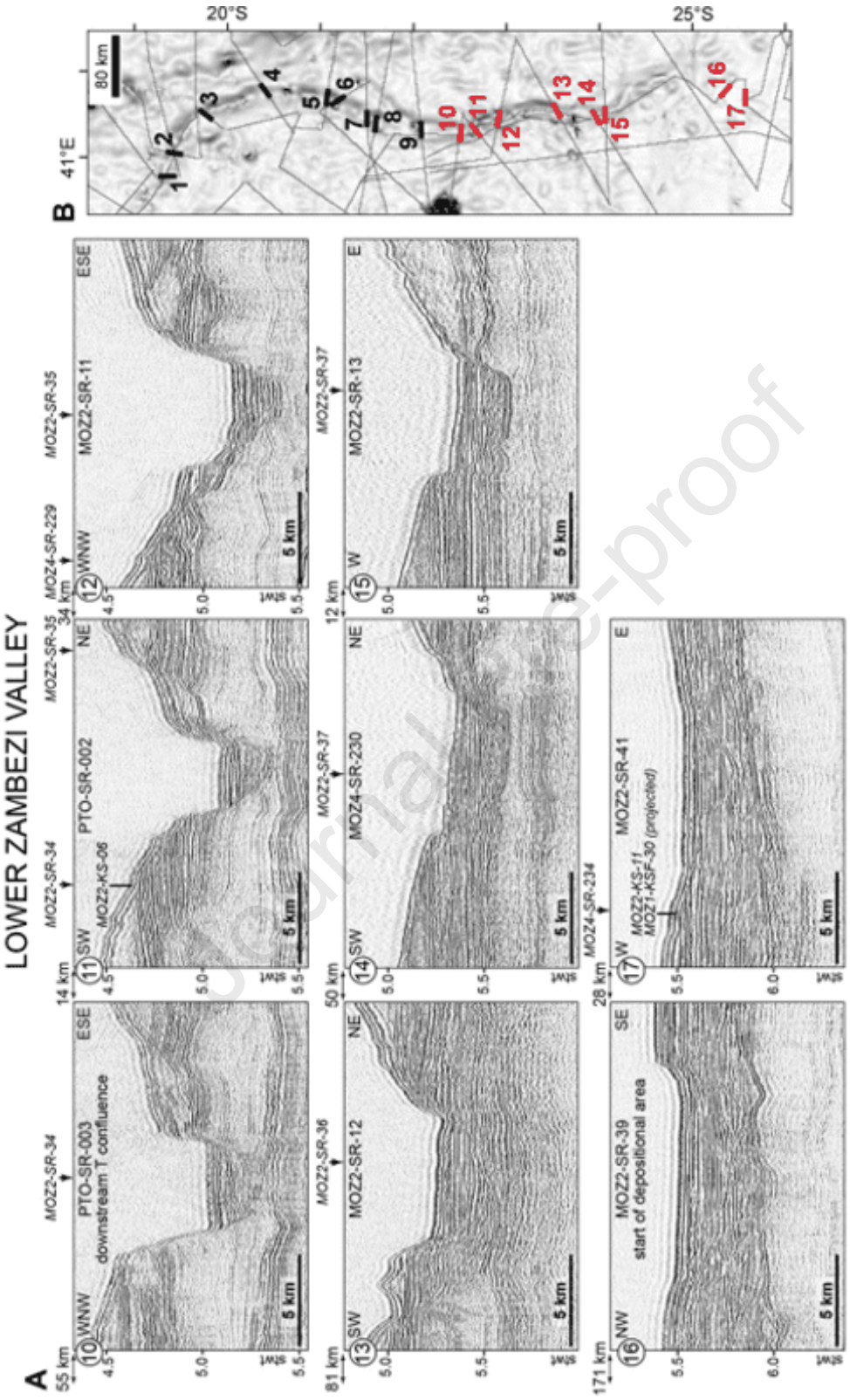

Supplementary material B-2: Uninterpreted seismic profiles of figure 19.

Highlights

- High-resolution seismic reflection data is used to investigate the Oligocene to present architectural evolution of the Zambezi depositional system.
- Five major depositional units are identified and demonstrate both turbiditic and contouritic deposits that occur most often synchronously.
- The Zambezi Fan is characterized by various episodes of incision that evidence multiple shifts of feeding axes since Oligocene.
- Progressive structural doming during Late Miocene caused a deep entrenchment of the Zambezi Valley.

Declaration of interests

☒ The authors declare that they have no known competing financial interests or personal relationships that could have appeared to influence the work reported in this paper.

☐The authors declare the following financial interests/personal relationships which may be considered as potential competing interests: